Acoustic Doppler Current Profiler

Principles of Operation

A Practical Primer

P/N 951-6069-00 (January 2011)

TELEDYNE
RD INSTRUMENTS
A Teledyne Technologies Company

Revision History:

January 2011 – Corrected Equation 9, page 34. Sound Speed ratio was inverted.

December 2006 – Added Phased Array Transducer section.

Teledyne RD Instruments

14020 Stowe Drive
Poway, California 92064

Phone +1 (858) 842-2600

FAX +1 (858) 842-2822

Sales – rdisales@teledyne.com

Field Service – rdifs@teledyne.com

Teledyne RD Instruments Europe

2A Les Nertieres
5 Avenue Hector Pintus
06610 La Gaude, France

Phone +33(0) 492-110-930

FAX +33(0) 492-110-931

Sales – rdie@teledyne.com

Field Service – rdiefs@teledyne.com

Client Services Administration – rdicsadmin@teledyne.com
Web: http://www.rdinstruments.com
24 Hour Emergency Support +1 (858) 842-2700

Table of Contents

1. Introduction 1
History of Teledyne RD Instruments 1
ADCP History 1
BroadBand ADCPs 2

2. The Doppler Effect and Radial Current Velocity 3
Sound 4
The Doppler Effect 5
How ADCPs use Backscattered Sound to Measure Velocity 6
The Doppler Effect Measures Relative, Radial Motion 8

3. BroadBand Doppler Processing 9
Doppler Time Dilation 9
Phase 10
Time Dilation and Doppler Frequency Shift 10
Phase Measurement and Ambiguity 11
Autocorrelation 12
Modes 12

4. Three-dimensional Current Velocity Vectors 13
Multiple Beams 13
Current Homogeneity in a Horizontal Layer 13
Calculation of Velocity with the Four ADCP Beams 13
Error Velocity: Why it is Useful 14
The Janus Configuration 14

5. Velocity Profile 15
Depth Cells 15
Regular Spacing of Depth Cells 15
Averaging Over the Range of Each Depth Cell 16
Range Gating 16
The Relationship of Range Gates and Depth Cells 16
The Weight Function for a Depth Cell 17

6. ADCP Data 18

7. Ensemble Averaging 20
ADCP Errors and Uncertainty Defined 20
Short-Term Versus Long-Term Uncertainty 21
The Approximate Size of Random Error and Bias 21
Beam Pointing Errors 21
Averaging Inside the ADCP Vs. Averaging Later 21
The Processing Cycle: Limitations on Averaging 22

8. ADCP Pitch, Roll, Heading and Velocity 23
Conversion from ADCP- to Earth- Referenced Current 23
Measuring ADCP Rotation and Translation 23
Self-Contained and Direct-Reading ADCPs 24

Data Correction Strategies for Self-Contained ADCPs....24
Vessel-mounted ADCPs....25
Synchros....26
Multiple Turn Synchros for Heading....26
Correction for Ship Velocity....26
Effects of Correction on Vessel-Mounted ADCP Measurements....27

9. Echo Intensity and Profiling Range....29
Sound Absorption....30
Beam Spreading....31
Source Level and Power....31
Scatterers....32
Bubbles....32

10. Sound Speed Corrections....33
Correction for Variation in Speed of Sound at the Transducer....33
Correcting Depth Cell Depth for Sound Speed Variations....34

11. Transducers....35
Transducer Beam Pattern....35
Transducer Clearance....37
Measurement Near the Surface or Bottom....38
Ringing....39
Pressure....40
Concave vs. Convex....40

12. Sound Speed and Thermoclines....41
Sound Speed Variation with Depth....41
Thermoclines....42

13. Bottom Tracking....43
Difference Between Bottom-Tracking and Water-Profiling....43
Implementation....44
Accuracy and Capability....44
Ice Tracking....44

14. Phased Array Transducer....45
Speed of sound considerations....46
Summary....47

15. Conclusion....47

16. Useful References....48

List of Figures

Figure 1. Doppler shift....3
Figure 2. Wave definitions....4
Figure 3. The Doppler effect....5

Figure 4. Typical ocean scatterers....6
Figure 5. Backscattered sound....6
Figure 6. Backscattered sound involves two Doppler shifts....7
Figure 7. The Doppler shift depends on radial motion....8
Figure 8. Relative velocity vector....8
Figure 9. Propagation delay and phase change....9
Figure 10. Time dilation and Doppler frequency shift....10
Figure 11. The echo from a single scatterer....11
Figure 12. The relationship of beam and earth velocity components....13
Figure 13. Non-homogeneous flow leads to large error velocity....14
Figure 14. ADCP depth cells compared with conventional current meters....15
Figure 15. Range-time plots....16
Figure 16. Range-time plot detail....16
Figure 17. Depth cell weight functions....17
Figure 18. View facing an ADCP transducer....18
Figure 19. The distribution of single-ping data....20
Figure 20. Steps in the ping processing cycle....22
Figure 21. ADCP tilt and depth cell mapping....23
Figure 22. Range-dependent signal attenuation....31
Figure 23. Typical beam pattern of a 150 kHz transducer....35
Figure 24. Keep obstructions out of the shaded region in front of the transducer....37
Figure 25. Transducer beam angle and the thickness of the contaminated layer at the surface....38
Figure 26. Concave and convex transducers....40
Figure 27. How sound speed variations with depth affects sound propagation....41
Figure 28. The effect of strong thermoclines on sound propagation....42
Figure 29. A long pulse is needed for the beams to ensonify (illuminate) the entire bottom all at once....43
Figure 30. Comparison of a multi-piston and a 2-dimensional phased array transducer....45
Figure 31. Comparison of a 600kHz phased array transducer with a 600kHz WorkHorse transducer....46

Notes

1. Introduction

This is the second edition of ***Acoustic Doppler Current Profiler Principles of Operation: A Practical Primer***. The first edition addressed narrowband Acoustic Doppler Current Profilers (ADCPs). Since then, Teledyne RD Instruments has introduced the *BroadBand ADCP*, and more recently the Work-horse, which uses BroadBand technology. This edition has been revised to reflect changes introduced with BroadBand technology.

This primer is a combination of both basic principles and practical information needed to understand how BroadBand ADCPs work and how they are used. The primer will address basic concepts for most of the principles presented, often treating them only superficially. For more in-depth study, we recommend use of the references listed in the Bibliography.

History of Teledyne RD Instruments

Teledyne RD Instruments, Inc., located in San Diego, CA, specializes in the design and manufacture of underwater acoustic Doppler products for a wide array of current profiling and precision navigation applications.

Originally founded as RD Instruments, the company was formed in 1982 by Fran Rowe and Kent Deines as a result of their development of the industry's first Acoustic Doppler Current Profiler (ADCP™), a revolutionary device capable of profiling currents at up to 128 individual points in the water column.

Through the years, RD Instruments experienced steady growth and remained dominant in the industry by providing an unwavering commitment to new product development, superior data quality, and the highest level of customer service and support.

In August 2005, RD Instruments was purchased by Teledyne Technologies, and now operates as a wholly owned indirect subsidiary of Teledyne Technologies, Inc. Upon acquisition, the company's name was changed to Teledyne RD Instruments.

The company currently employs over 200 multi-disciplined scientists, engineers, technicians, sales, and support personnel; and resides in a 30,000 square foot ISO-9001:2000 facility that includes state-of-the art engineering, laboratory, manufacturing, and test areas.

ADCP History

The predecessor of ADCPs was the Doppler speed log, an instrument that measures the speed of ships through the water or over the sea bottom. The first commercial ADCP, produced in the mid-1970's, was an adaptation of a commercial speed log (Rowe and Young, 1979). The speed log was redesigned to measure water velocity more accurately and to allow measurement in range cells over a depth profile. Thus, the first vessel-mounted ADCP was born.

In 1982, TRDI produced its first ADCP, a self-contained instrument designed for use in long-term, battery-powered deployments (Pettigrew, Beardsley and Irish, 1986). In 1983, TRDI produced its first

vessel-mounted ADCP. By 1986, TRDI had five different frequencies (75-1200 kHz) and three different ADCP models (self-contained, vessel-mounted, and direct-reading).

Doppler signal processing has evolved with the instruments over the years. Speed logs used relatively simple processing with phase locked loops or similar methods. Such processing is still used in some commercial speed logs today. The first generation of ADCPs used a narrow-bandwidth, single-pulse, autocorrelation method that computes the first moment of the Doppler frequency spectrum. This method was the first to produce water velocity measurements with sufficient quality for use by oceanographers. It has since been superseded by BroadBand signal processing, an even more accurate method.

BroadBand ADCPs

In 1991, TRDI began shipping its first production prototype BroadBand ADCPs. The BroadBand method (patents 5,208,785 and 5,343,443) enables ADCPs to take advantage of the full signal bandwidth available for measuring velocity. Greater bandwidth gives a BroadBand ADCP far more information with which to estimate velocity. With typically 100 times as much bandwidth, BroadBand ADCPs reduce variance nearly 100 times when compared with narrowband ADCPs. Where appropriate, these differences will be noted.

2. The Doppler Effect and Radial Current Velocity

This section introduces the Doppler effect and how it is used to measure relative radial velocity between different objects. We will begin by developing the basic mathematical equation that relates the Doppler shift with velocity.

The *Doppler effect* is a change in the observed sound pitch that results from relative motion. An example of the Doppler effect is the sound made by a train as it passes (Figure 1). The whistle has a higher pitch as the train approaches, and a lower pitch as it moves away from you. This change in pitch is directly proportional to how fast the train is moving. Therefore, if you measure the pitch and how much it changes, you can calculate the speed of the train.

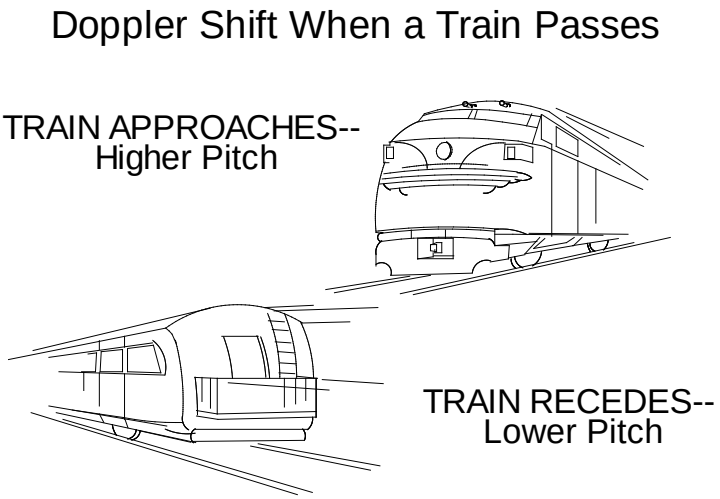

Figure 1. When you listen to a train as it passes, you hear a change in pitch caused by the Doppler shift.

Sound

Sound consists of pressure waves in air, water or solids. Sound waves are similar in many ways to shallow-water ocean waves. With help from Figure 2, following are some definitions we will use:

- Waves – Water wave crests and troughs are high and low water elevations. Sound wave "crests" and "troughs" consist of bands of high and low air pressure.
- Wavelength – The distance between successive wave crests.
- Frequency – The number of wave crests that pass per unit time.
- Speed of sound – The speed at which waves propagate, or move by, where;

$$\text{Speed of sound} = \text{frequency} \times \text{wavelength}$$

$$C = f \lambda \qquad \text{(Equation 1)}$$

(Example, 1500 m/s = 300,000 Hz × 5 mm)

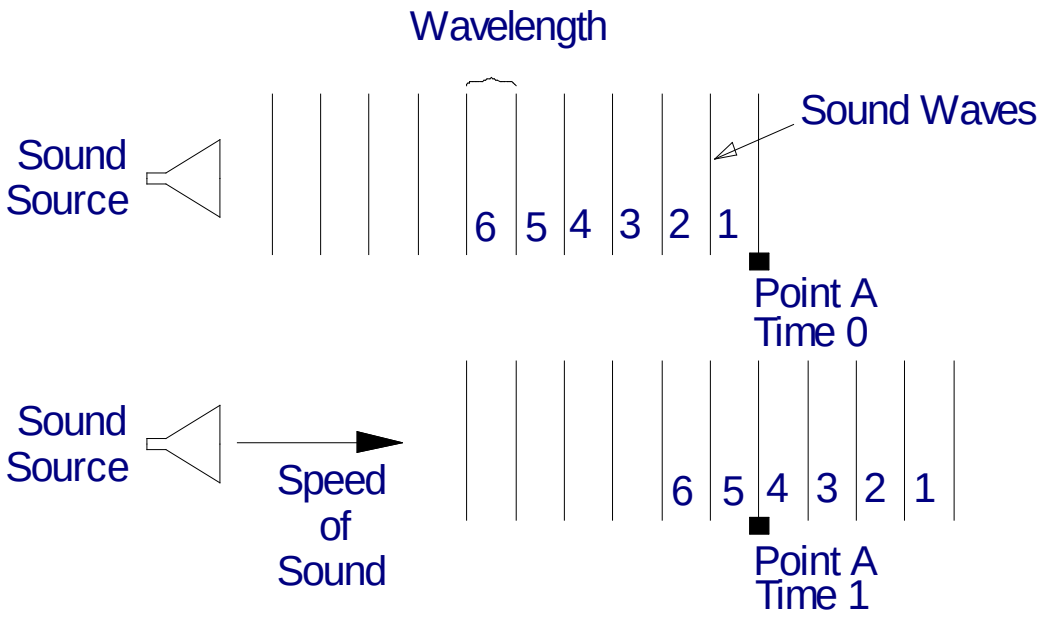

Figure 2. Wave definitions

The Doppler Effect

Imagine you are next to some water, watching waves pass by you (Figure 3). While standing still, you see eight waves pass in front of you in a given interval (Figure 3a). Now, if you start walking toward the waves (Figure 3b), more than eight waves will pass by in the same interval. Thus, the wave frequency appears to be higher. If you walk in the other direction, fewer than 8 waves pass by in this time interval, and the frequency appears lower. This is the Doppler effect.

The Doppler shift is the difference between the frequency you hear when you are standing still and what you hear when you move. If you are standing still and you hear a frequency of 10 kHz, and then you start moving toward the sound source and hear a frequency of 10.1 kHz, then the Doppler shift is 0.1 kHz.

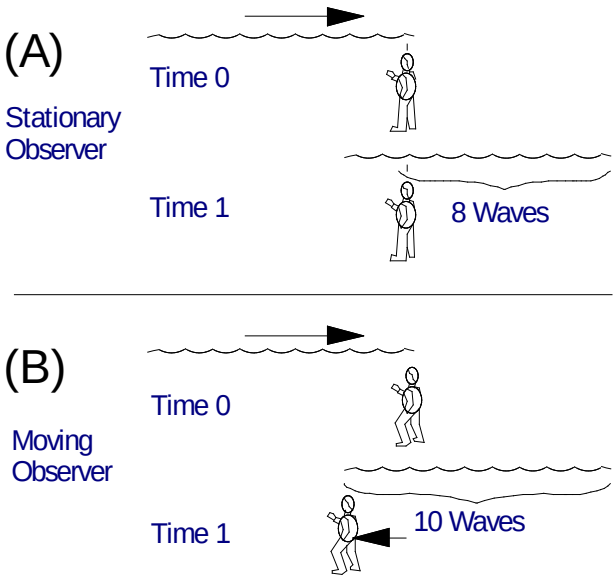

Figure 3. The Doppler effect. An observer walking into the waves will see more waves in a given time than will someone standing still.

The equation for the Doppler shift in this situation is:

$$F_d = F_s(V/C) \qquad \text{(Equation 2)}$$

Where:

- F_d is the Doppler shift frequency.
- F_s is the frequency of the sound when everything is still.
- V is the relative velocity between the sound source and the sound receiver (the speed at which you are walking toward the sound; m/s).
- C is the speed of sound (m/s).

Note that:

- If you walk faster, the Doppler shift increases.
- If you walk away from the sound, the Doppler shift is negative.
- If the frequency of the sound increases, the Doppler shift increases.
- If the speed of sound increases, the Doppler shift decreases.

How ADCPs use Backscattered Sound to Measure Velocity

ADCPs use the Doppler effect by transmitting sound at a fixed frequency and listening to echoes returning from sound scatterers in the water. These sound scatterers are small particles or plankton that reflect the sound back to the ADCP. Scatterers are everywhere in the ocean. They float in the water and *on average they move at the same horizontal velocity as the water* (note that this is a key assumption!). Figure 4 shows some examples of typical scatterers in the ocean.

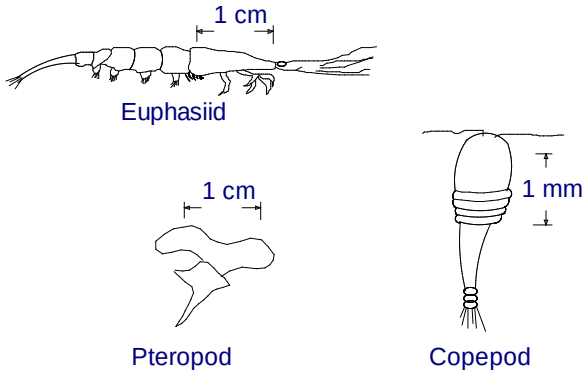

Figure 4. Typical ocean scatterers

Sound scatters in all directions from scatterers (Figure 5). Most of the sound goes forward, unaffected by the scatterers. The small amount that reflects back is Doppler shifted.

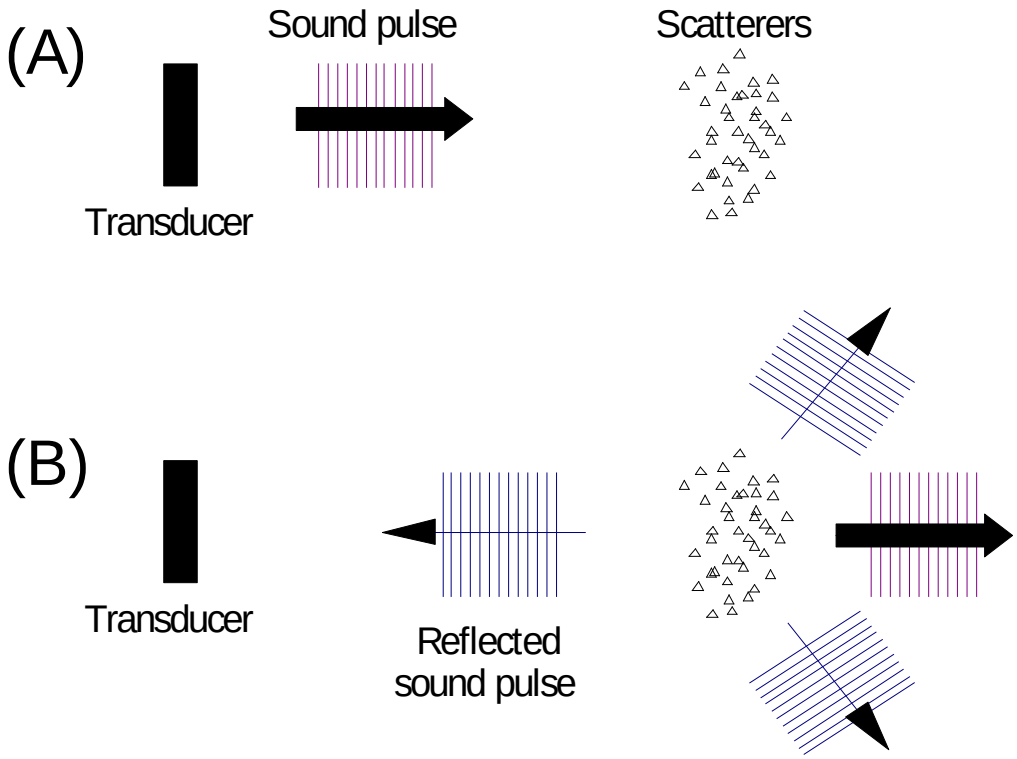

Figure 5. Backscattered sound. (A) Transmitted pulse; (B) A small amount of the sound energy is reflected back (and Doppler shifted), most of the energy goes forward.

When sound scatterers move away from the ADCP, the sound they hear is Doppler-shifted to a lower frequency proportional to the relative velocity between the ADCP and scatterer (Figure 6a). The backscattered sound then appears to the ADCP as if the scatterers were the sound source (Figure 6b); the ADCP hears the backscattered sound Doppler-shifted a second time.

Therefore, because the ADCP both transmits and receives sound, the Doppler shift is doubled, changing (2) to:

$$F_d = 2\ F_s(V/C) \qquad \text{(Equation 3)}$$

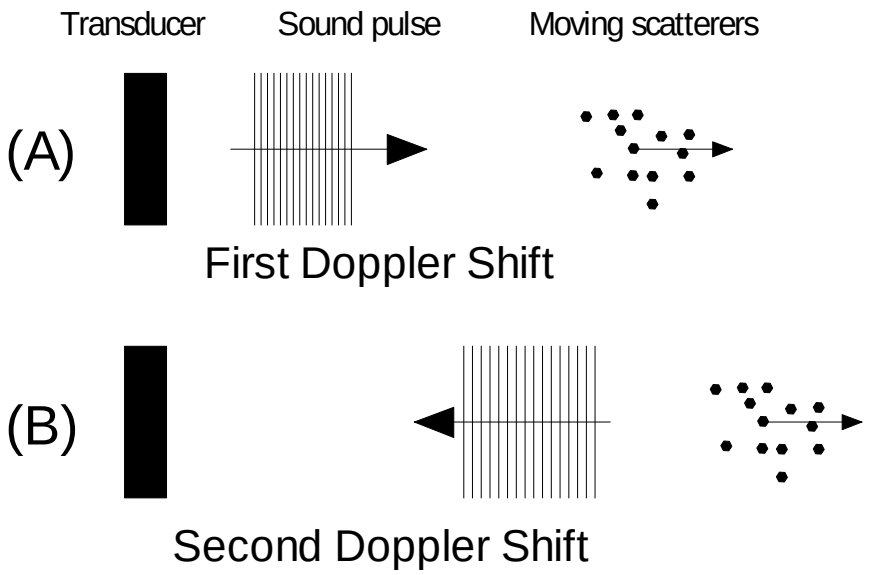

Figure 6. Backscattered sound involves two Doppler shifts, (A) one enroute to the scatterers, and (B) a second on the way back after reflection.

The Doppler Effect Measures Relative, Radial Motion

The Doppler shift only works when sound sources and receivers get closer to or further from one another – this is radial motion. On the other hand, angular motion changes the direction between the source and receiver, but not the distance separating them. Thus angular motion causes no Doppler shift. The different effects of angular and radial motion on the Doppler shift are shown in Figure 7.

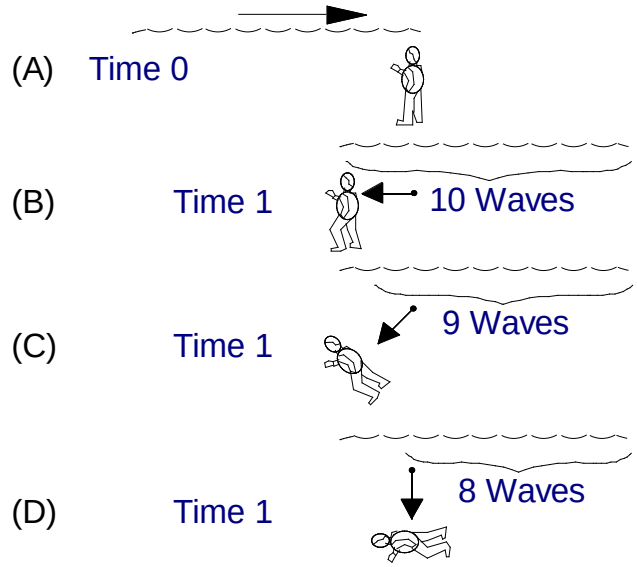

Figure 7. The Doppler shift depends on radial motion only. Observer A is standing still and sees no Doppler shift. Observers B, C, and D are all moving at the same speed. Observer B is moving toward the source (i.e. radially) and sees the largest Doppler shift. In contrast, observer D is moving perpendicular (i.e. angularly) to the source and sees no Doppler shift at all. Observer C is moving part radially and part angularly and sees less Doppler shift than observer B.

Limiting the Doppler shift to the radial component only adds a new term, *cos*(*A*), to (3):

$$F_d = 2\, F_s (V/C) \cos(A) \qquad \text{(Equation 4)}$$

where *A* is the angle between the relative velocity vector and the line between the ADCP and scatterers (Figure 8).

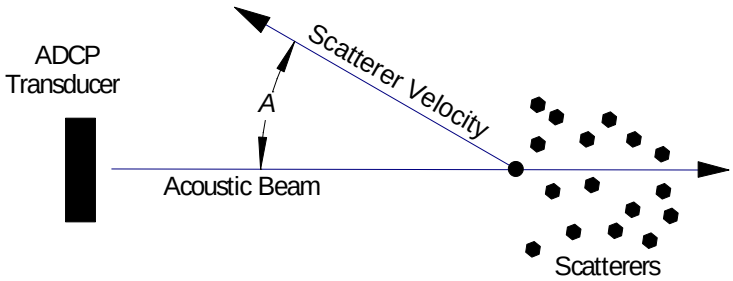

Figure 8. Relative velocity vector. The ADCP measures only the velocity component parallel to the acoustic beams. A is the angle between the beam and the water velocity.

3. BroadBand Doppler Processing

So far, we have looked at Doppler processing in terms of changes in frequency. BroadBand Doppler processing, while equivalent mathematically, is easier to understand in terms of *time dilation*, that is, in terms of changes to the signal in time rather than frequency. This section introduces the principles of BroadBand signal processing.

Doppler Time Dilation

To understand time dilation, consider sound scattering from a single particle. The echo from a pulse of sound transmitted toward this particle will always look the same as long as the particle does not move. This result is illustrated in Figure 9A. If you move the particle a little further from the transmitter (Figure 9B), you will see that it takes a little longer for the sound to go back and forth. If you move the particle even more, it will take even longer (Figure 9C). This change in travel time caused by changing the distance traveled is called the *propagation delay*.

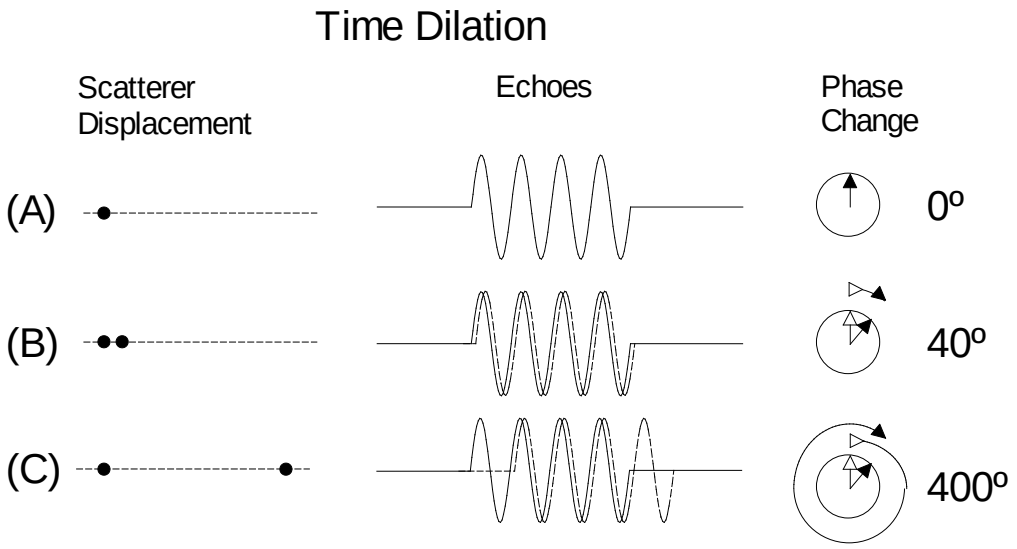

Figure 9. Propagation delay and phase change caused by scatterer displacement. Echoes are delayed when particles are farther from the sound source — this is called propagation delay. Propagation delay changes the relative phase of the echo.

Echoes from a single particle always look the same when the particle stays still — there is no propagation delay. Echoes have the same relative phase which means zero phase change.

Two echoes superimposed: the second echo takes longer to return because the particle was further away, hence it is delayed relative to the first echo. The delayed echo, shown with a dashed line, has a phase delay, relative to the first echo, of around 40º.

The second echo is delayed about 10 times as much as it was in example (B) because the particle moved about 10 times as far. The longer propagation delay corresponds to a phase change of around 400º.

The *principle of time dilation* is simple: sound takes longer to travel back and forth when particles are further away from the transducer. A change in travel time, or a propagation delay, corresponds to a change in distance. If you measure the propagation delay, and if you know the speed of sound, you can tell how far the particle has moved. If you know the time lag between sound pulses, you can compute the particle's velocity.

Phase

Phase is a convenient and precise means to measure propagation delay. BroadBand ADCPs use phase to determine time dilation. To understand phase consider the hands of a clock. One revolution of the hour hand corresponds to 360º of phase. One complete cycle (the time from one peak to the next) of a sinusoidal signal corresponds to 360º of phase. Hence, the phase differences between the first and second echoes shown in Figure 9 are roughly (A) 0º, (B) 40º, and (C) 400º. These phase differences are exactly proportional to the particle displacements.

Time Dilation and Doppler Frequency Shift

Figure 10 shows that frequency shift and time dilation are equivalent. Figure 10A shows the echo from two closely-spaced pulses returning from a stationary particle. If instead, the particle moves away from the transducer (Figure 10B), the time between the pulse echoes increases. This is because by the time the second pulse arrives at the particle, the particle has moved further from the transducer; it therefore takes longer for the sound to travel back and forth.

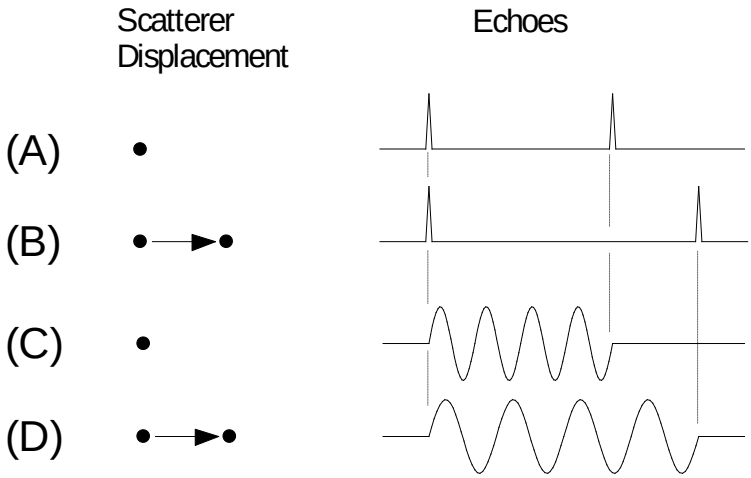

Figure 10. Time dilation and Doppler frequency shift. (A) and (B) compare echoes of pulse pairs from stationary and moving particles. (C) and (D) show the same for the echo from a sinusoidal pulse with a duration equal to the time between the two short pulses in (A) and (B). The dashed lines indicate that the stretching is the same for the two pulses as it is for he sinusoid.

The same effect applies to a sinusoidal pulse (Figs. 10C and 10D). By the time the end of the sinusoidal pulse reaches the particle, the particle has moved further. This stretches the echo, changes the pitch of the echo, and thus causes a Doppler shift.

Many Doppler sonars measure frequency shift directly. BroadBand ADCPs use time dilation by measuring the change in arrival times from successive pulses. In reality, even though different measurement methods involve different approaches, they are often mathematically equivalent. TRDI engineers use phase to measure time dilation instead of measuring frequency changes because phase gives them a more precise Doppler measurement.

Phase Measurement and Ambiguity

The problem with phase measurement is that phase can only be measured in the range 0-360º. Once phase passes 360º, it starts over again at 0º. As far as an electronic phase measurement circuit is concerned, phases of 40º and 400º (400º = 360º + 40º) are the same.

To understand this, again consider the hands of a clock. If a clock had only a minute hand, you could measure time with a precision of about one minute, but you would not know which hour it was. On the other hand, if you had only an hour hand, you would know unambiguously which hour it was, but your time precision would be much coarser than a minute. To obtain precise measurements of velocity, the engineer wants phase measurements to be sensitive to changes in velocity much like the minute hand is sensitive to changes in time. But then she must devise a way to do the equivalent of counting hours in a clock. The parallel to the minute hand rotating around the clock is phase passing through multiples of 360º.

This process, figuring out how many times phase has passed 360º, is called *ambiguity resolution*. If echoes were as simple as those in Figure 9, it would not be hard to find simple ways to resolve phase ambiguity, but, as Figure 11 shows, the typical echo is complicated.

There are several ways to solve this problem. One is to keep the time between pulses so small that the particle never has enough time to move very far. If it cannot move very far, then phase will not change very much. This is like relying on the hour hand alone to tell time. In fact, the measurement precision gained with long time lags makes it attractive to accept ambiguous phase measurements (as in the clock's minute hand). This means that BroadBand ADCPs must also implement methods to resolve ambiguity.

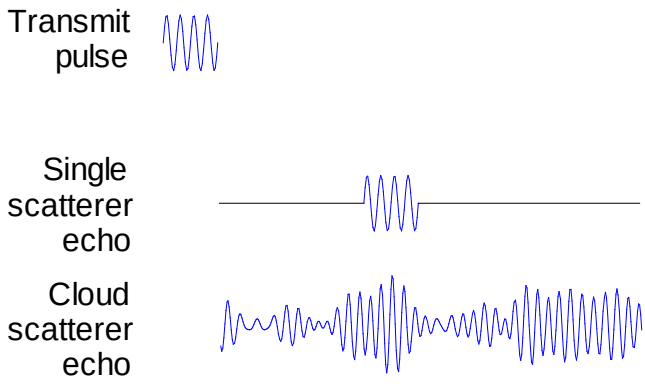

Figure 11. The echo from a single scatterer looks just like the transmit pulse, but the echo from a cloud of scatterers is complicated.

Autocorrelation

Autocorrelation is a mathematical method useful for comparing echoes. While autocorrelation involves complicated mathematics, what it accomplishes is simple. Well-correlated echoes look the same and uncorrelated echoes look different. Autocorrelation is an efficient and effective method for detecting small phase changes.

TRDI uses an autocorrelation method to process complicated real-world echoes to obtain velocity. By transmitting a series of coded pulses, all in sequence inside a single long pulse, we obtain many echoes from many scatterers, all combined into a single echo. We extract the propagation delay by computing the autocorrelation at the time lag separating the coded pulses. The success of this computation requires that the different echoes from the coded pulses (all buried inside the same echo) be correlated with one another.

Modes

ADCPs implement a variety of modes with varying time lags and pulse forms. Default modes are chosen for robustness and measurement precision. Other modes are often able to produce even more robust measurements (useful, for example, in highly turbulent water) or more precise measurements. Modes that produce highly precise measurements may work only in limited environmental conditions. They can also be more likely to fail when, for example, flow becomes rapid or turbulent.

4. Three-dimensional Current Velocity Vectors

The discussion so far has addressed single acoustic beams which can only measure a single velocity component, the component parallel to the beam. This section explains how an ADCP uses four beams to obtain velocity in three dimensions plus additional redundant (yet nevertheless useful) information. To use multiple beams to obtain velocity in three dimensions, one must assume that currents are uniform (homogeneous) across layers of constant depth.

Multiple Beams

When an ADCP uses multiple beams pointed in different directions, it senses different velocity components. For example, if the ADCP points one beam east and another north, it will measure east and north current components. If the ADCP beams point in other directions, trigonometric relations can convert current speed into north and east components. A key point is that one beam is required for each current component. Therefore, to measure three velocity components (e.g. east, north, and up), there must be at least three acoustic beams.

Current Homogeneity in a Horizontal Layer

One problem with using trigonometric relations to compute currents is that the beams make their measurements in different places. If the current velocities are not the same in the different places, the trigonometric relations will not work. Currents must be horizontally homogeneous, that is, they must be the same in all four beams. Fortunately, in the ocean, rivers, and lakes, horizontal homogeneity is normally a reasonable assumption.

Calculation of Velocity with the Four ADCP Beams

Figure 12 illustrates how we compute three velocity components using the four acoustic beams of an ADCP. One pair of beams obtains one horizontal component and the vertical velocity component. The second pair of beams produces a second, perpendicular horizontal component as well as a second vertical velocity component. Thus there are estimates of two horizontal velocity components and two estimates of the vertical velocity. Figure 12 shows the beams oriented east/west and north/south, but the orientation is arbitrary.

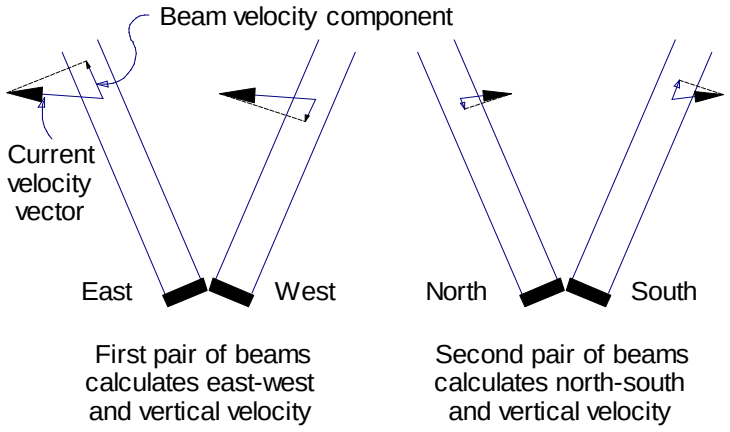

Figure 12. The relationship of beam and earth velocity components

Error Velocity: Why it is Useful

The *error velocity* is the difference between the two estimates of vertical velocity. Error velocity depends on the data redundancy: only three beams are required to compute three dimensional velocity. The fourth ADCP beam is redundant, but not wasted. Error velocity allows you to evaluate whether the assumption of horizontal homogeneity is reasonable. It is an important, built-in means to evaluate data quality.

Figure 13 shows two different situations. In the first situation, the current velocity at one depth is the same in all four beams. In the second, the velocity in one beam is different. The error velocity in the second case will, on average, be larger than the error velocity in the first case. Note that it does not matter whether the velocity is different because the ADCP beam is bad or because the actual currents are different. Error velocity can detect errors due to inhomogeneities in the water, as well as errors caused by malfunctioning equipment.

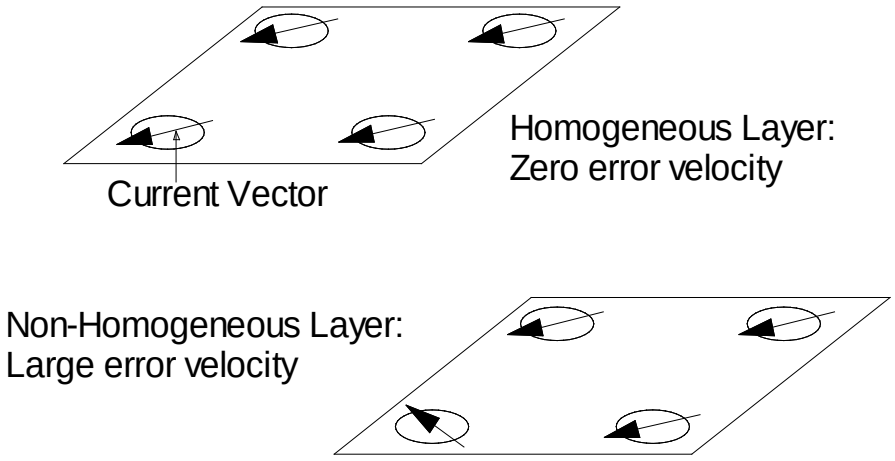

Figure 13. Non-homogeneous flow leads to large error velocity.

The Janus Configuration

The ADCP transducer configuration is called the Janus configuration, named after the Roman god who looks both forward and backward. The Janus configuration is particularly good for rejecting errors in horizontal velocity caused by tilting (pitch and roll) of the ADCP. This is because:

- The two opposing beams allow vertical velocity to cancel when computing horizontal velocity.
- Pitch and roll uncertainty causes single-beam velocity errors proportional to the sine of the pitch and roll error. Beams in a Janus configuration reduce these velocity errors to second order; that is, velocity errors are proportional to the square of the pitch and roll errors.

5. Velocity Profile

The most important feature of ADCPs is their ability to measure current profiles. ADCPs divide the velocity profile into uniform segments called depth cells (depth cells are often called bins). This section explains how profiles are produced and some of the factors involved.

Depth Cells

Each depth cell is comparable to a single current meter. Therefore an ADCP velocity profile is like a string of current meters uniformly spaced on a mooring (Figure 14). Thus, we can make the following definitions by analogy:

- Depth cell size = distance between current meters
- Number of depth cells = number of current meters

There are two important differences between the string of current meters and an ADCP velocity profile. The first difference is that the depth cells in an ADCP profile are always uniformly spaced while current meters can be spaced at irregular intervals. The second is that the ADCP measures average velocity over the depth range of each depth cell while the current meter measures current only at one discrete point in space.

Regular Spacing of Depth Cells

Regular spacing of velocity data over the profile makes it easier to process and interpret the measured data. This regular spacing is comparable to a regular sample rate. It is much more difficult to process irregularly-sampled data than it is to process data sampled uniformly in time. The same benefit applies to measurements in a vertical profile.

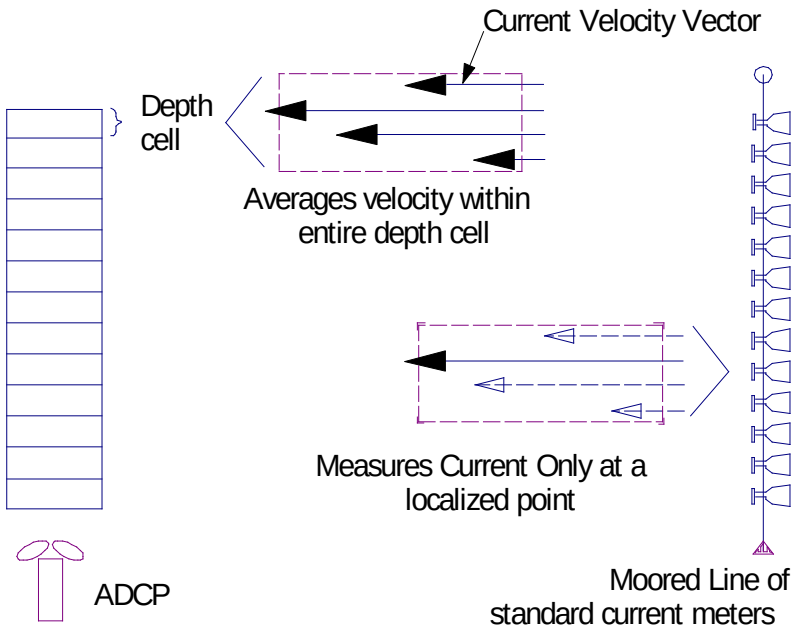

Figure 14. ADCP depth cells compared with conventional current meters

Averaging Over the Range of Each Depth Cell

Unlike conventional current meters, ADCPs do not measure currents in small, localized volumes of water. Instead, they average velocity over the depth range of entire depth cells. This averaging reduces the effects of spatial aliasing. Aliasing in time series causes high frequency signals to look like low frequency signals. The effect is equivalent over depth. Smoothing the observed velocity over the range of the depth cell rejects velocities with vertical variations smaller than a depth cell, and thus reduces measurement uncertainty.

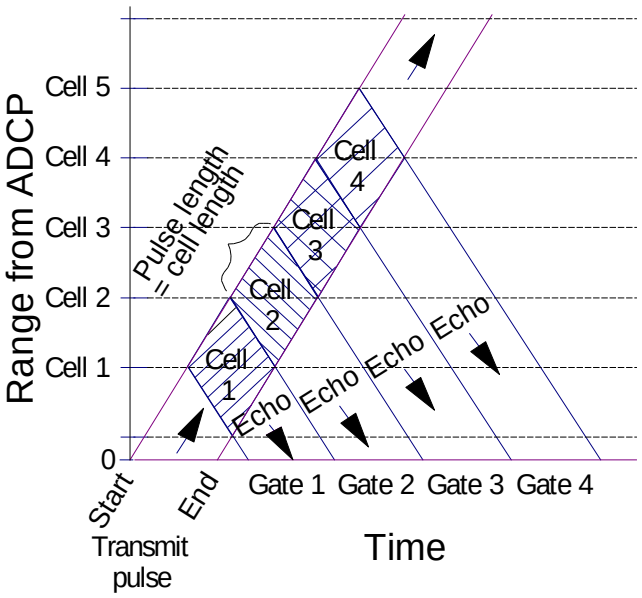

Figure 15. Range-time plots shows how transmit pulses and echoes travel through space. Time starts at the beginning of the transmit pulse and range starts at the transducer face.

Range Gating

Profiles are produced by range-gating the echo signal. Range gating breaks the received signal into successive segments for independent processing. Echoes from far ranges take longer to return to the ADCP than do echoes from close ranges. Thus, successive range gates correspond to echoes from increasingly distant depth cells.

The Relationship of Range Gates and Depth Cells

A depth cell averages velocity over a range within the water column, but the averaging is usually not uniform over this range. Instead, the depth cell is most sensitive to velocities at the center of the cell and least sen sitive at the edges. The remainder of this section explains why this happens and describes the resulting *weight function*.

Figure 15 illustrates the relationship of range gates and depth cells. This plot relates time and distance from the ADCP. At the left side of the time axis is the transmit pulse. Transmit pulse propagation is shown with lines sloping up and to the right. Echo propagation back to the transducer is shown with lines sloping down and to the right.

As time increases, the transmit pulse propagates away from the ADCP. Immediately after the transmit pulse is complete, the ADCP turns off the transducer and waits for a short time called the *blank period.* The ADCP now starts processing the echo corresponding to Range Gate 1. When Gate 1 is complete, the ADCP immediately begins processing Gate 2, and so on. These steps are shown on the horizontal axis.

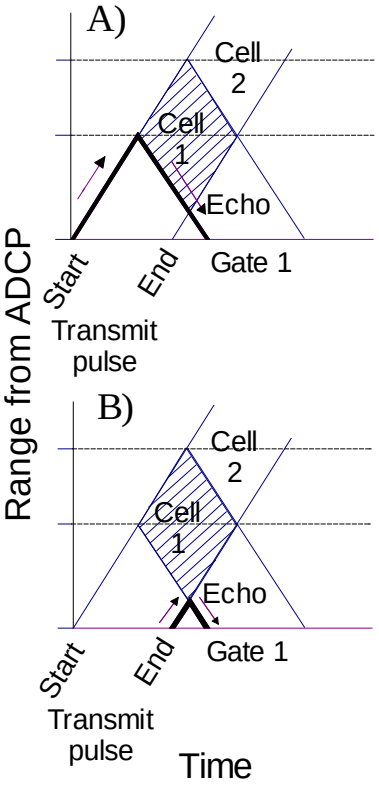

Figure 16. Range-time plot detail

To understand how Figure 15 works, first consider the echo of the leading edge of the transmit pulse from a scatterer located at the center of Cell 1. Follow the propagation line that marks the leading edge of the transmit pulse — *this line slopes up from the origin*. Now find the line corresponding to the echo — *this line slopes down from the intersection of the transmit pulse leading edge and the center of Cell 1*. These lines, shown in detail in Figure 16A, trace the passage of the leading edge of the transmit pulse to the scatterer and the echo of this leading edge back to the transducer face. Figure 16B traces the passage of the trailing edge of the transmit pulse to a different scatterer and its echo back to the transducer. Both echoes arrive at the transducer at the beginning of Range Gate 1.

Once you understand the concepts presented in the previous paragraph, you can trace and study the propagation paths that outline Cell 1. You can learn how the center of Cell 1 contributes the largest fraction of the echo signal to Range Gate 1. The echo from the farthest part of Cell 1 contributes signal only from the leading edge of the transmit pulse. The echo from the closest part of Cell 1 contributes signal only from the trailing edge of the transmit pulse. You can also see how adjacent cells overlap each other.

The Weight Function for a Depth Cell

Scatterers in the center of the diamond-shaped space-time areas in Figure 15 contribute more energy to the signal in Range Gate 1 than do scatterers near the top or bottom of the diamond. This means they play a larger role in determining the average current velocity measured in Gate 1. The velocity in each depth cell is a weighted average using the triangular *weight functions* in Figure 17. Note that each depth cell overlaps adjacent depth cells. This overlap causes a correlation between adjacent depth cells of about 15%.

The above weight function applies to most normal situations for both narrowband and BroadBand ADCPs. However, when the transmit pulse and depth cell sizes are different, the shape of the weight function changes. For example, if the transmit pulse were short relative to the cell size, the weight function would be approximately rectangular with little overlap over adjacent cells. If the transmit pulse were longer than the depth cell, cells would overlap even more, and the data would be smoothed across depth cells.

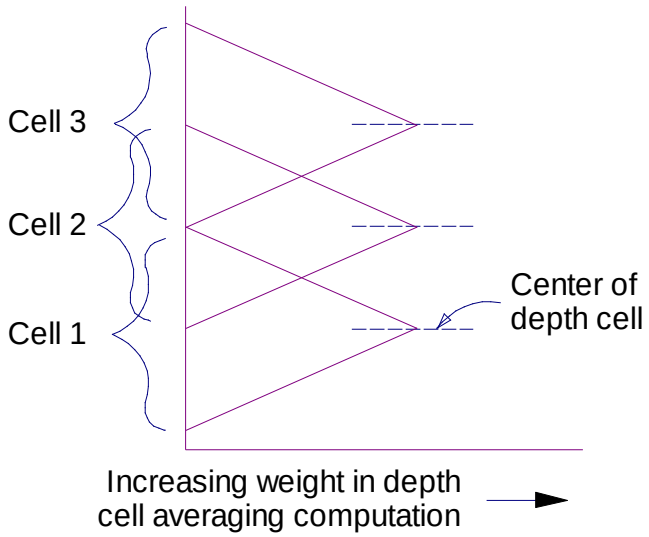

Figure 17. Depth cell weight functions: depth cells are more sensitive to currents at the center of the cell than at the edges

6. ADCP Data

This section introduces and describes the data produced by a BroadBand ADCP. This data includes the following four different kinds of standard profile data:

- Velocity
- Echo intensity
- Correlation
- Percent good

Velocity data are output in units of mm/s. Depending on your requirements, you can record data in one of the following formats:

- *Beam coordinates* — Velocity is output parallel to each beam.
- *Earth coordinates* — Velocity is converted into north, east and up components.
- *ADCP coordinates* — Similar to earth coordinates except that velocity is converted to forward, sideways, and up components, relative to the ADCP. ADCP forward is the direction toward which beam 3 faces. ADCP sideways is to the right of forward. Figure 18 shows the typical layout of a four-beam ADCP. Keep in mind that the view is looking at the face of the ADCP. Beam 2 of a downward-looking convex ADCP points in the direction of a positive sideways velocity. Vertical velocities are positive upwards.
- *Ship coordinates* — Similar to ADCP coordinates except that heading is rotated into ship's forward and sideways. If beam 3 faces toward the bow of the ship, ADCP and ship coordinates are the same.

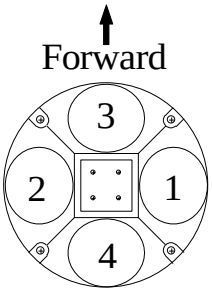

Figure 18. View facing an ADCP transducer. The layout is the same for both convex and concave transducers (see Figure 26).

Velocity transformations from beam coordinates to earth coordinates are described in more detail in the section entitled ADCP movement: pitch, roll, heading, and velocity.

Echo intensity data are output in units proportional to decibels (dB). Data are obtained from the receiver's received signal strength indicator (RSSI) circuit.

Correlation is a measure of data quality, and its output is scaled in units such that the expected correlation (given high signal/noise ratio, S/N) is 128.

Percent-good data tell you what fraction of data passed a variety of criteria. Rejection criteria include low correlation, large error velocity and fish detection (false target threshold). Default thresholds differ for each ADCP; each threshold has an associated command.

Bottom-track data are not profile data and they are output in a different part of the data structure, but their format is similar to the velocity profile data. The bottom-track coordinate transformation is identical to the one used for the water profile. Bottom-track output also includes the vertical component of the distance, along each beam, to the bottom.

7. Ensemble Averaging

Single-ping velocity errors are too large to meet most measurement requirements. Therefore, data are averaged to reduce the measurement uncertainty to acceptable levels. This section defines ADCP uncertainties, averaging methods, and the effect of averaging on data uncertainty.

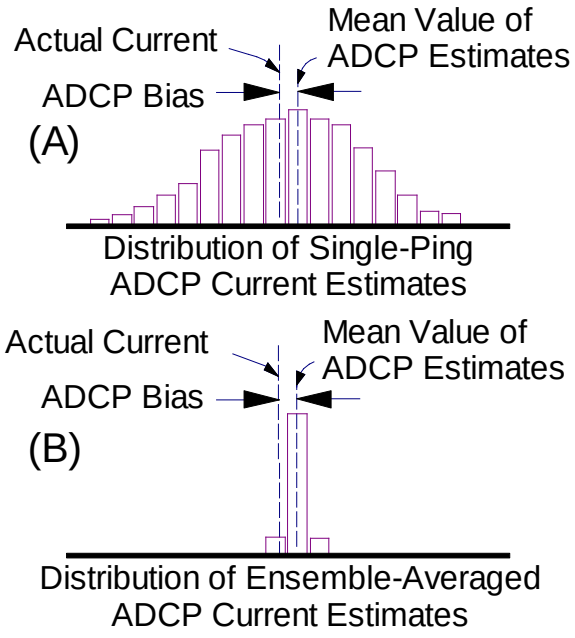

Figure 19. The distribution of single-ping data (A) compared with the distribution of 200-ping averages of the same data (B).

ADCP Errors and Uncertainty Defined

Velocity uncertainty includes two kinds of error — random error and bias. Averaging reduces random error but not bias.

Figure 19 shows these errors with two example distributions of ADCP current estimates. Assume that the distribution in Figure 19A was computed from 20,000 measurements of exactly the same current. In this distribution, the measurements cluster around the actual value of the current, but there is variation due to the random error. Note also that the overall average is different from the actual current. Bias causes this difference.

Because random error is uncorrelated from ping to ping, averaging reduces the standard deviation of the velocity error by the square root of the number of pings, or:

$$\text{Standard Deviation} \propto N^{-1/2} \qquad \text{(Equation 5)}$$

Where N is the number of pings averaged together.

The distribution in Figure 19B shows what might happen if we were to make 200 ensembles of 100 pings each from the original 20,000 pings. Averaging the 100 pings in each ensemble reduces the random error of each ensemble by a factor of about 1/10. This is clear in the smaller spread of the lower distribution. Note that the average value of both distributions is the same and that both are different from the actual current. This difference, which does not go away with averaging, is the measurement bias.

An important point is that averaging can reduce the relatively large random error present in single-ping data, but that, after a certain amount of averaging, the random error becomes smaller than the bias. At this point, further averaging will do little to reduce the overall error.

Short-Term Versus Long-Term Uncertainty

Short-term uncertainty is defined as the error in single-ping ADCP data. Short-term uncertainty is dominated by random error.

Long-term uncertainty is defined as the error present after enough averaging has been done to essentially eliminate random error. Long-term error is the same as bias.

The Approximate Size of Random Error and Bias

ADCP single-ping random error or short-term error can range from a few mm/s to as much as 0.5 m/s. The size of this error depends on internal factors such as ADCP frequency, depth cell size, number of pings averaged together and beam geometry. External factors include turbulence, internal waves and ADCP motion.

Random error in narrowband ADCPs is relatively easy to estimate, but it is harder to estimate for BroadBand ADCPs. This is because BroadBand measurements have more adjustable parameters, each of which affects uncertainty. Because random errors generated internally in the ADCP are typically an order of magnitude smaller than in a comparable narrowband ADCP, external random error sources (i.e. turbulence) can dominate internal ADCP errors.

You can estimate random errors by computing the standard deviation of the error velocity. This is because random errors are independent from beam to beam and because the error velocity is scaled by the ADCP to give the correct magnitude of horizontal-velocity random errors. To predict the size of internal random errors, consult brochure specifications or use one of the various software tools that TRDI provides for this purpose.

Bias is typically less than 10 mm/s. This bias depends on several factors including temperature, mean current speed, signal/noise ratio, beam geometry, etc. It is not yet possible to measure ADCP bias and to calibrate or remove it in post-processing.

Beam Pointing Errors

Beam pointing errors can be a dominant source of velocity bias. A beam pointing error is uncertainty in the beam direction. Standard manufacturing practice introduces errors into beam angles. Depending on measurement requirements and the care with which the transducer elements were installed, these errors could introduce unacceptable bias. The as-installed beam angles are measured in the manufacturing process and stored in the BroadBand ADCP's memory. These angles modify the coordinate conversion matrix which corrects for beam pointing errors when converting from beam to earth velocity coordinates.

Averaging Inside the ADCP Vs. Averaging Later

An ADCP system can calculate ensemble averages inside the ADCP, in the data acquisition system, or in both. It is possible, for example, to average ensembles of several pings in the ADCP and to send the results to a computer which then computes averages of these ensembles. Normally, unless there is a good reason to do otherwise, the best rule is to let the ADCP convert data into earth coordinates and to average data into ensembles before transmitting them out. Following is a list of the factors that might affect your choice of where to average your data.

- Vector averaging — Conversion to earth coordinates prior to averaging allows the ADCP to compute true vector averages.
- Beam pointing errors are automatically corrected when the ADCP converts from beam to earth coordinates, thus minimizing related biases.
- Data transmission takes time and can slow down ping processing. Averaging reduces the time required for data transmission.

The Processing Cycle: Limitations on Averaging

Averaging is limited by the ping rate, which is limited by how fast the ADCP can collect, process and transmit data. Figure 20 shows a typical data collection cycle inside the ADCP. Each ping has five phases: overhead, transmit pulse, blank period, processing, and sleep. The overhead time is used to wake up the ADCP, initialize and process various subsystems (e.g. the clock, compass, etc.) and to prepare for ping processing. After pulse transmission and a short delay to allow the transducer to ring down (see later), the ADCP begins to process the echo. When echo processing is complete, the ADCP either goes to sleep to conserve battery power or immediately begins another data collection cycle. After all the pings are collected, the ADCP computes an ensemble average and transmits the data to the internal data recorder, to an external data acquisition system, or to both. When the ADCP pings rapidly, data transmission runs in the background, using CPU time when it is free.

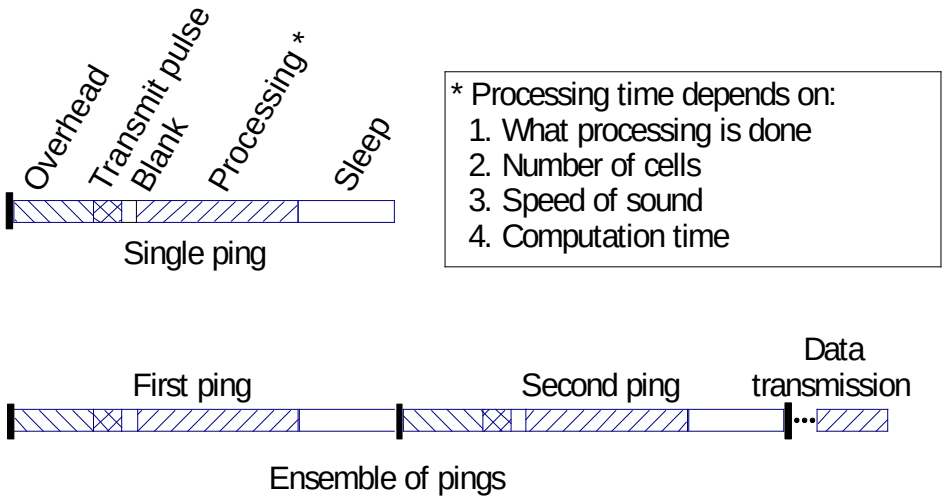

Figure 20. Steps in the ping processing cycle

8. ADCP Pitch, Roll, Heading and Velocity

ADCPs measure currents relative to the ADCP. The ADCP itself can be oriented arbitrarily and moving relative to the earth. Therefore, it is usually necessary to correct the data for ADCP attitude and motion. This section covers why ADCP data require correction and how to measure and correct for ADCP motion and attitude.

There are two kinds of motion that require correction — rotation (pitch, roll, and heading) and translation (ship velocity).

Conversion from ADCP- to Earth- Referenced Current

The following are three general steps in the conversion from ADCP- referenced currents to earth- referenced currents

Step 1. ADCPs measure velocity parallel to the four acoustic beams (beam coordinates). These data are converted into an orthogonal coordinate system of ADCP north, east, and up. This correction adjusts for the angle of the beams (trigonometry) as well as the fact that depth cells of a tilted ADCP (Figure 21) move up and down relative to one another. Correction includes the following:

- *Trigonometry*. The beam angle used or correction (see Eq. 4) is the sum of the ADCP beam mounting angle (i.e. 20º) plus (or minus) the tilt angle.
- *Depth cell mapping*. To ensure horizontal homogeneity, the calculated velocity at a particular depth uses cells that are at the same depth. Figure 21B shows the depth cells of a tilted ADCP. Note, for example, that depth cell 4 on the left beam is at the same depth as depth cell 6 on the right beam. Depth cell mapping matches these two cells together to compute earth velocity at this depth. (Note: depth cell mapping was implemented for BroadBand firmware versions 5.0 and later.)

Step 2. The ADCP rotates velocity components into true (or magnetic) east and north (earth coordinates). This correction requires heading data.

Step 3. ADCP velocity relative to the earth is subtracted, providing absolute, earth-referenced currents. This correction requires measurements of the ship's velocity relative to the earth. Subtraction is normally done after the data are collected and recorded.

In practice, these steps are not always done in the above order, and they are not necessarily separated into discrete steps.

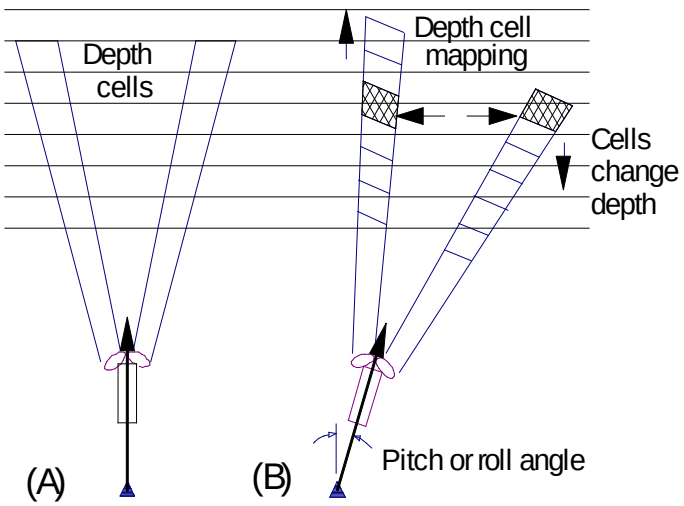

Figure 21. ADCP tilt and depth cell mapping

Measuring ADCP Rotation and Translation

There are many ways to measure rotation and translation. The following are com-

monly used with ADCPs:

Rotation (heading)
1. Flux-gate compass
2. Gyrocompass

Rotation (pitch and roll)
1. Inclinometers
2. Vertical gyro

Translation
1. Bottom-tracking
2. Navigation device (i.e. GPS)
3. Assume a "layer of no motion" (reference layer)

Self-Contained and Direct-Reading ADCPs

Self-Contained and Direct-Reading ADCPs are designed for use where motion is relatively slow and unaffected by surface waves. In such an environment a flux-gate compass and inclinometers can effectively measure pitch, roll, and heading. These sensors are used because of their small size (they fit inside the ADCP pressure case) and low power consumption (necessary for Self-Contained ADCPs). These sensors have the following limitations:

Flux-gate compasses cannot be used near ferrous materials, such as a ship's steel hull, that would affect the earth's magnetic field. Some flux-gate compasses are noisy when affected by accelerations of surface waves.

Inclinometers measure tilt relative to earth gravity, but cannot differentiate the acceleration of gravity from accelerations caused, for example, by surface waves. Hence, inclinometers can be noisy in moving boats.

Both BroadBand and Workhorse compasses are sensitive to motions, either directly (as in the BroadBand compass) or indirectly through their inclinometers.

Data Correction Strategies for Self-Contained ADCPs

Self-Contained ADCPs can be mounted on moorings where they are free to change orientation, or in frames on the sea bottom where their orientation is fixed. These two methods call for different data correction strategies.

Moored ADCPs should convert each ping into earth coordinates prior to averaging. This ensures that ensemble averages are vector averages. Earth-coordinate averaging is equivalent to vector-averaging in standard single-point current meters, and it ensures that the data have both the best accuracy and highest resolution possible given the depth cell size.

When an ADCP is mounted on the sea bottom, you could choose to record data either in beam coordinates or in earth coordinates. Recording data in earth coordinates reduces the time and effort required for post-processing and it ensures that beam pointing angles are properly corrected. Recording data in beam coordinates allows you to record the least-processed data, and it allows them to optimize the

processing used to convert the data to earth coordinates. However, proper correction for beam pointing angle errors can be time-consuming to implement and debug.

Correction for beam pointing angle errors is more important for the Workhorse than for the Broad-Band because the Workhorse manufacturing process allows wider tolerances for transducer installation. Without correction, errors can be significant.

Vessel-mounted ADCPs

The remainder of this section applies to vessel-mounted ADCPs in which the transducer is permanently installed on the hull. It applies equally to direct-reading ADCPs that are temporarily mounted on the hull. Procedures used once at the time of installation of a standard vessel-mounted ADCP must be followed each time a direct-reading ADCP is reinstalled on a ship.

Gyrocompasses and vertical gyros are used on ships because they are unaffected by horizontal accelerations from surface waves. Inclinometers are sometimes used in ships, but it is not good practice to use the raw inclinometer data to correct each ping. Instead, the average pitch and roll may be used to detect variation in mean tilts caused by changes in ballasting, propeller speed, etc.

There are many different ways for ADCPs to obtain attitude information from gyros, but this flexibility is limited by the need to obtain tilt and heading at exact times during ping processing. Most often, ADCPs use a synchro interface to measure pitch, roll and heading angles. ADCPs also obtain heading information through a stepper interface.

Direct-reading ADCP deck boxes with synchro interfaces send their data to the ADCP via a serial interface using a proprietary format. TRDI does not yet support sending attitude data into an ADCP using industry-standard formats, but some software programs (i.e. TRANSECT) can accept serial attitude data in NMEA formats. Keep in mind that, while ships often digitize attitude on a regular time interval (e.g. every second or ten seconds), the ADCP has no control over data sampling and therefore cannot synchronize the attitude data with the pings.

Synchros

A synchro interface enables ADCPs to get heading data at the exact time it is required. Synchros are motors that are normally used in pairs. When one synchro rotates a given amount, the other rotates the same amount. The synchro interface uses five wires for the following synchro outputs:

- Three "sense" outputs — S1, S2, and S3
- Two "reference" outputs — R1 and R2

The outputs have AC voltages that vary depending on the synchro rotation angle. The synchro voltage is expressed as the maximum voltage between any pair of sense outputs. Synchros are commonly powered by 110 VAC, in which case the maximum voltage between sense outputs will be 90 VAC. This is a 90-volt synchro. Standard synchro voltages include:

- 90 VAC
- 26 VAC
- 11.8 VAC

Other voltages are rarely used, but the ADCP synchro interface can work with any voltage between 11.8 and 90 VAC. Adjustment is made by changing the value of a precision resistor network in the interface. The frequency of a synchro can have an average value between 50 and 1000 Hz.

Multiple Turn Synchros for Heading

It is common for gyrocompasses to use multiple-turn synchros for output. For example, a multiple-turn synchro with a 360:1 turns ratio would rotate 360 times every time the ship rotates once. Common turns ratios are:

- 360:1
- 90:1
- 36:1
- 1:1

TRDI's synchro interface uses any of the above. If the turns ratio is other than 1:1, the ADCP must initialize the synchro interface to the correct starting direction. For example, with a 36:1 synchro, the synchro makes one complete revolution each time the ship turns 10º. The ADCP cannot tell the difference between 313, 13, 23, etc. This means the operator must set the ADCP system for the correct angle when the ADCP starts up. This is most easily handled via a panel interface on either the direct-reading or vessel-mounted ADCP deck boxes.

It is normally best to use a 1:1 synchro interface whenever possible for the following reasons:

- The accuracy of a 1:1 synchro is normally sufficient.
- If power is lost, synchro turns ratios other than 1:1 require reinitialization.

Pitch and roll synchros must use 1:1 turns ratios.

Correction for Ship Velocity

When available, absolute ship velocity is recorded along with the water velocity profiles. Later, during post-processing, the ship velocity can be subtracted from the current profile data. There are three ways to measure ship velocity:

1. Bottom-tracking
2. Navigation
3. Assuming a "layer of no motion" (reference layer)

Bottom-tracking can only be used when the bottom is within the ADCP's bottom-tracking range — this is about 1.5 times the normal profiling range. When bottom-tracking is unavailable, *navigation* can be used to estimate ship velocity. Trade-offs of the various kinds of navigation systems are discussed below.

Using a *reference layer* involves assuming that a layer within the profiling range of an ADCP has no motion. The utility of this assumption depends upon the site where the measurements are made.

Effects of Correction on Vessel-Mounted ADCP Measurements

This section covers the following two kinds of motion that limit a vessel-mounted ADCP's data quality:

- Pitch and roll motions of the ship in surface waves
- The large ship speed compared with the measured currents.

It turns out that pitch and roll are of less concern than one might think. Kosro (1985) used an ADCP to measure currents and a gyro to measure pitch and roll on a ship offshore northern California. He recorded raw ADCP pings along with simultaneous gyro data, and then computed current profiles both with and without pitch and roll correction. He found the following results:

- Corrected and uncorrected horizontal currents were different with a bias of about 1 cm/s. The uncorrected data were also smoothed over a depth range about equal to the distance that depth cells moved up or down as a result of the pitch and roll.
- Corrected and uncorrected vertical currents were different by as much as 5 cm/s.

Therefore, we conclude that pitch and roll correction is required only in the following circumstances:

- When the greatest possible data accuracy is required.
- When the ship is expected to encounter severe wave conditions.
- When accurate vertical velocity components are required.

Correction of ADCP data for the speed of the ship can vary from relatively easy to quite difficult. The easiest correction is when bottom-track data are available. Correction with bottom-tracked ship velocity is relatively easy to do well because:

- Bottom-track velocity data are usually more accurate than the current profile data.
- The bottom-track velocity and current profile velocity are measured in the same coordinate system.

Bottom-tracking's biggest advantage is that many of its largest errors are matched by exactly the same errors in the current profile. These *common-mode* errors then cancel exactly when bottom-track velocity is subtracted from the current profile data. Major common-mode errors include compass errors and velocity biases caused by beam pointing errors. This advantage arises from the fact that bottom-tracking and current profiling use the same coordinate system

In contrast, ship's navigation and current profiling share no common-mode errors. For example, errors of 1º or more are common in ship's gyros. A 1º compass error introduces a sideways velocity error of almost 10 cm/s when a ship steams at 5 m/s.

Heading errors are caused by the following:

- *Transducer misalignment.* This is a result of the difficulty in measuring the orientation of the transducer in the ship. In fact, the transducer need not be oriented in any specific direction, but the orientation must be known. For more information on *in-situ* transducer orientation calibration, refer to Pollard and Read (1989) or Joyce (1988).
- *Gyro errors and instability.* This depends on the make and model of the gyrocompass. One source of error is the Schuler oscillation, a direction error with a period of 84 minutes and an amplitude of typically 0.5º—1.0º. The Schuler oscillation is often excited when the ship makes a turn.

The accuracy of navigation correction depends strongly on the navigation used. Differential GPS is generally the best choice for overall accuracy and easy use. However, bottom-tracking usually produces smaller short-term errors than even the best GPS.

9. Echo Intensity and Profiling Range

Echo intensity is a measure of the signal strength of the echo returning from the ADCP's transmit pulse. Echo intensity is sometimes used to survey the concentration of zooplankton or suspended sediment. TRDI has not yet developed procedures for absolutely calibrating BroadBand backscatter measurements, but BroadBand ADCPs (including Workhorses) are useful for relative measurements. This section introduces some of the factors involved in interpreting and using backscatter data.

Echo intensity depends on:

- Sound absorption
- Beam spreading
- Transmitted power
- Backscatter coefficient

An approximate equation for echo intensity is:

$$EI = SL + SV + constant - 20\log(R) - 2\alpha R \qquad \text{(Equation 6)}$$

Where:

EI is the echo intensity (dB)
SL is the source level or transmitted power (dB)
SV is the water-mass volume backscattering strength (dB)
α is the absorption coefficient (dB/meter)
R is the distance from the transducer to the depth cell (meters)

The constant is included because the measurement is relative rather than absolute. This means the ADCP sees variations in echo intensity, but it cannot make absolute measurements that can be compared with other ADCPs. The term 2eR accounts for absorption and 20log(R) accounts for beam spreading.

Keep in mind that the relationship of echo intensity to particle concentration strongly depends on the particle size. This means that you must calibrate the relationship between echo intensity and concentration with *in-situ* measurements. When the particle size distribution is variable, it may not be possible to satisfactorily calibrate this relationship.

The maximum range of the ADCP corresponds to the location where the signal strength drops to levels comparable to the noise level. Beyond this range the ADCP cannot accurately calculate Doppler shifts. The remainder of this section will review factors that affect both the signal strength as a function of range from the ADCP and the overall range of the ADCP.

Sound Absorption

Absorption reduces the strength of echoes as a result of physical and chemical processes in water. Absorption in the ocean is more rapid than in fresh water, primarily because of chemical reactions. Absorption causes a linear reduction (proportional to 2eR above) of echo intensity with range when measured in dB. This means that absorption causes echo intensity to decay exponentially with increasing range.

Sound absorption (in dB/meter) increases roughly in proportion to frequency within the frequency range in which ADCPs operate (75-1200 kHz; see Table 1 or Urick, 1983). This produces an inverse relationship between frequency and range.

Table 1. Sound absorption (At 4°C, 35‰ and at sea level) and nominal profiling range of a BroadBand ADCP. The transmit power listed is the maximum power that can be transmitted subject to limitations caused by shock formation.

Frequency (kHz)	α(dB/m)	Nominal Range (m)	@ Power (W)
76.8	0.022-0.028	700	250
153.6	0.039-0.050	400	250
307.2	0.062-0.084	120	80
614.4	0.14-0.20	60	30
1228.8	0.44-0.66	25	15

The sound absorption values given in Table 1 come from Urick (1983) and Kinsler, et al. (1980). The range shown more likely represents uncertainty in the true absorption rather than the actual variation present in the ocean.

Beam Spreading

Beam spreading is a geometric cause for echo attenuation as a function of range. In Equation 6 above, beam spreading is represented as a logarithmic loss in echo intensity with increasing range, where echo intensity is measured in dB. In linear units, the echo intensity decreases proportional to the range squared.

An explanation for this range-squared behavior is shown in Figure 22. Doubling the distance to a scatterer causes the scatterer to intersect one-quarter as much of the total sound energy in the beam. Thus, it reflects back one-quarter as much energy. However, because the beam has four times the area, there will be four times as many scatterers reflecting sound back, keeping the total reflected energy constant. The reduction in echo intensity is the result of the transducer intersecting only one-quarter as much of the total reflected energy as before.

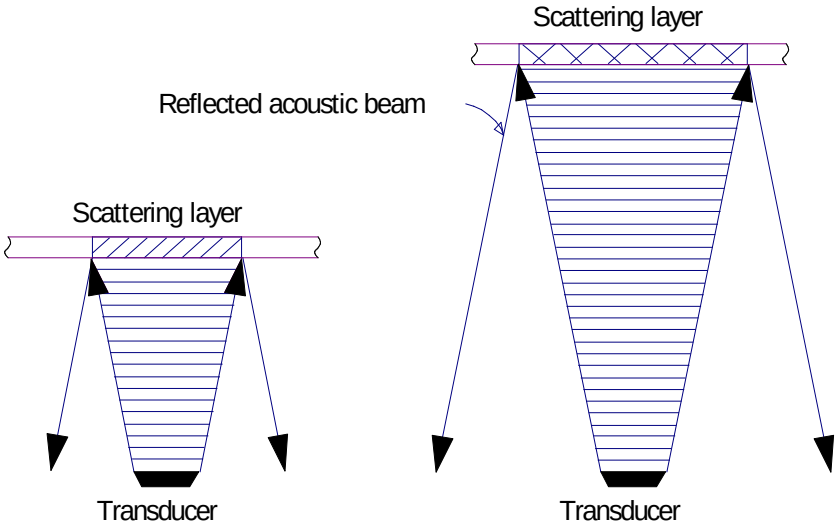

Figure 22. Range-dependent signal attenuation

Source Level and Power

The source level of a BroadBand signal depends on the following factors:

- *Power*. The ADCP's transmit power is normally proportional to the square of the transmit voltage. The primary difference between low and high-power ADCPs is the voltage applied to the transducer. If the voltage is regulated (i.e. in high-power BroadBands), the transmit power going into the transducer stays constant. The transmit power of a Workhorse ADCP, however, is taken directly from its DC input. Thus, its transmit power is proportional to the square of the input voltage. Transmit power also depends on stored energy. High-power BroadBand ADCPs use large banks of capacitors to supply power for long bottom-track pulses. If the ADCP has insufficient capacitance, the power falls while the pulse is being transmitted.
- *Transducer efficiency*. The transducer controls transmit power through its efficiency. Typical efficiencies range from 25-80%.

- *Transmit pulse*. Longer transmit pulses put more energy into the water. In addition, pulse coding can reduce the average power transmitted. Codes normally just switch phase (by multiplying by ±1) but otherwise sustain constant power. However, the average power can be reduced by using codes that include zeros instead of only ±1.
- *Shock*. As sound intensity increases, it reaches a point where it becomes nonlinear. Non-linear acoustics (shock formation) rapidly attenuates sound, effectively reducing energy to levels near the maximum possible without shock formation. Shock formation tends to limit transmit energy primarily at 300 kHz and above.
- *Cavitation*. At lower frequencies (150 kHz and below), large amplitude acoustic pressure fluctuations cause pressures so low that vapor bubbles form momentarily. These bubbles collapse noisily, seriously degrading ADCP performance. Cavitation is a problem primarily on fast-moving ships.

Scatterers

The concentration of scatterers affects range because more scatterers reflect more sound. The dominant oceanic sound scatterer at ADCP frequencies is zooplankton with sizes on the order of one millimeter (Figure 4 shows some typical zooplankton). Other scatterers can include suspended sediment, detritus, and density gradients (though density gradients are relatively weak scatterers).

On occasion, the lack of scatterers in the water reduces the range relative to the nominal range. In one extreme example, the range was about one-third of the nominal range (on a cruise by the Institute of Ocean Sciences, Wormley, UK, using an RD-VM0150 near Mauritius). Such instances have been uncommon, occurring less than 10% of the time.

ADCPs used at depths below 1200 m often experience range reductions to as little as one-third normal range.

Bubbles

In rough seas, breaking waves generate bubbles below the ocean surface. When bubbles pass under the ship's hull, they can act as a shield, inhibiting the transmission of sound. Bubbles sometimes reduce profiling range, and in extreme cases, bubbles block the signal completely.

10. Sound Speed Corrections

An ADCP computes sound speed based on an assumed salinity and transducer depth and on the temperature measured at the transducer. The ADCP uses this sound velocity to convert velocity data into engineering units and to compute distances along the beams. The sound speed is recorded along with the other ADCP data. This section describes corrections you may make for sound speed variations and errors.

Correction for Variation in Speed of Sound at the Transducer

Velocity data are output in units of mm/s. The velocity scale factor is proportional to the speed of sound measured at the transducer. The ADCP automatically computes sound speed given the measured temperature and an assumed salinity. If it is in error (i.e. if the assumed salinity is wrong), velocity can be corrected for sound speed in post processing by using the following equation:

$$V_{corrected} = V_{uncorrected} (C_{real}/C_{ADCP}) \quad \text{(Equation 7)}$$

where C_{real} is the true sound speed at the transducer and C_{ADCP} is the sound speed recorded by the ADCP.

You may use the following equation to compute sound speed (Urick, 1983):

$$C = 1449.2 + 4.6T - 0.055T^2 + 0.00029T^3 + (1.34 - 0.01T)(S - 35) + 0.016D \quad \text{(Equation 8)}$$

Where:

T is the temperature in ºC
S is salinity in parts per thousand (‰)
D is the depth in meters

Variations in sound speed with depth (e.g. away from the transducer) do not affect calibration, as will be shown later.

Correcting Depth Cell Depth for Sound Speed Variations

The ADCP computes depth cell locations by assuming that the sound speed is constant over the water column. In so doing, the ADCP automatically accounts for the transducer beam angle (20º or 30º).

When range is large and sound speed differs from the speed at the transducer, the depth of each depth cell may be corrected if the sound speed profile is known. One procedure for doing this consists of the following steps:

- Determine the position of the first depth cell
- Determine the length of the depth cell using the equation:

$$L_{corrected} = L_{uncorrected} (C_{real} / C_{ADCP}) \quad \text{(Equation 9)}$$

Where L is the depth cell length.

- Using the above depth cell length, determine the position of the next depth cell.
- Repeat this process for all depth cells.

11. Transducers

Transducer quality is essential for data quality. ADCPs place unusually high demands on transducers. They must be directional (including both narrow beamwidth and suppressed side lobes) and efficient. BroadBand processing requires 25-50% bandwidth, and deep deployments require that the transducer withstand extreme pressures. This section describes transducer characteristics, particularly those that affect measurement performance.

The active elements in transducers are piezoelectric ceramic disks that expand or contract under the influence of an electric field. The electric field is applied through thin layers of silver deposited on the surfaces of the ceramic. When a voltage is applied, the disk gets thicker or thinner, depending on the polarity of the voltage.

The ceramic disk is potted (encased) with polyurethane in a metal cup with a reflective backing material. Self-Contained ADCPs are designed for high pressure, using an incompressible backing material so that the transducer will not break under pressure.

Transducer Beam Pattern

The transducer beam pattern shows the strength of transmitted sounds far from the transducer as a function of the angle. The angle is measured relative to the transducer axis, a line drawn from the center of the transducer perpendicular to the transducer face. The beam pattern is reciprocal in that it represents equally well the transducer's sensitivity to incoming sound as a function of direction.

Figure 23 shows an example transducer beam pattern. The main lobe points in the direction of the transducer axis, defined to be 0º. Most of the energy passes through the main lobe. The beamwidth is the width of the main lobe at the -3 dB level (-3 dB corresponds to half the signal strength).

Side lobes point in directions different from the main lobe. Outside of 15º from the main lobe, side lobes are suppressed by typically 35 dB or more relative to the main lobe. The size of the side lobes depends on the size of the transducer as well as the details of its manufacture. If the transducer is larger (at a given frequency), the beam becomes narrower, and side lobes are suppressed.

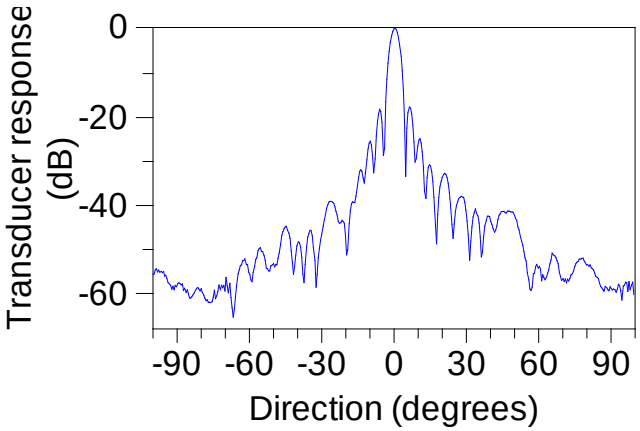

Figure 23. Typical beam pattern of a 150 kHz transducer. Transducer response is one-way, measured relative to the response at the transducer axis.

Some side lobes do not depend on transducer size, but result instead from modes of vibration in the piezoelectric ceramic. It is common to find side lobes at about 40º from the main lobes, and these side lobes can be dominant error sources.

The transducer beam pattern shown in Figure 23 is a one-way beam pattern because it shows the strength of the transmitted sound. The sensitivity of the transducer to echoes is characterized by

two-way transducer beam patterns because the transducer both transmits and receives sound. The two-way beam pattern is simply double (in dB) the one-way beam pattern. Therefore side lobes that are suppressed by 40 dB in the one-way pattern are suppressed by 80 dB in the two-way pattern. Energy reflected from these directions is suppressed by a factor of 100,000,000 relative to the main lobe.

Table 2 lists dimensions and characteristics of some of TRDI's transducers.

Table 2. Characteristics of some typical Broadband ADCP transducers

Frequency (kHz)	Wavelength (mm)	Transducer diam. (mm)	Beamwidth at -3dB	Avg. Side lobe level
76.8	20	280	5.0°	.36 dB
153.6	10	165	4.0°	.36 dB
307.2	5	133	2.2°	.41 dB
614.4	2.5	101	1.5°	.42 dB
1228.8	1.25	54	1.4°	.42 dB

Transducer Clearance

Obstructions in front of transducers can interfere with the acoustic beams and degrade data quality. Figure 24 shows the region in which you must eliminate all obstructions.

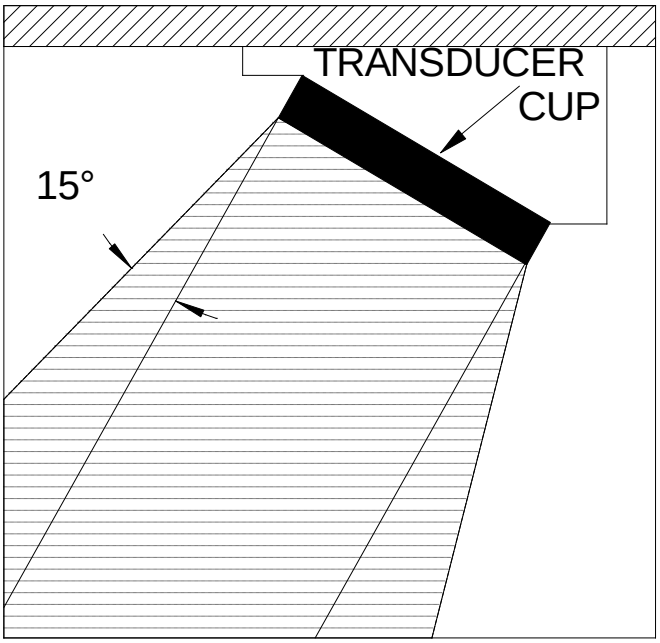

Figure 24. Keep obstructions out of the shaded region in front of the transducer. This region includes a 15º cone around the transducer.

Measurement Near the Surface or Bottom

The echo from a hard surface such as the sea surface or bottom is so much stronger than the echo from scatterers in the water that it can overwhelm the side lobe suppression of the transducer. You should normally reject data from distances too close to the surface (when looking up) or bottom (when looking down). Figure 25 shows transducer beam angles oriented 20º and 30º from vertical. For the 20º transducer, the echo through the side lobe facing the surface returns to the ADCP at the same time as the echo from the main lobe at 94% of the distance to the surface. This means data from the last 6% of the range to the surface can be contaminated. The concept is the same for a 30º transducer except that contamination covers a greater fraction of the range (15%). The effect is the same for an ADCP at the surface looking down to the bottom.

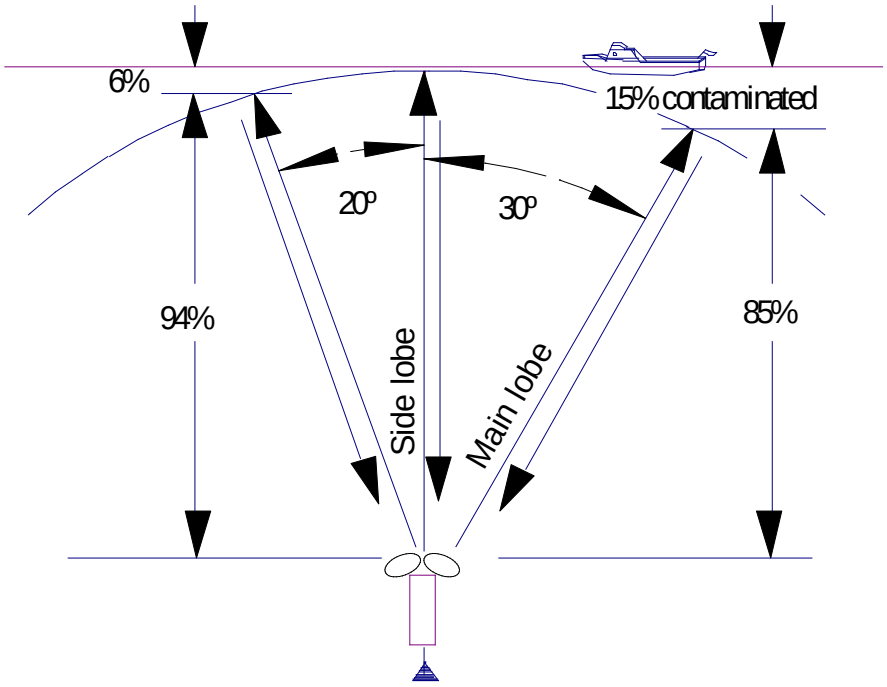

Figure 25. The relationship between transducer beam angle and the thickness of the contaminated layer at the surface.

The equation that governs this is:

$$R_{max} = D \cos(\theta) \qquad \text{(Equation 10)}$$

Where:

R_{max} is the maximum range for acceptable data
D is the distance from the ADCP to the surface or bottom (as appropriate)
Angle θ is the angle of the beam relative to vertical (normally 20º or 30º)

When looking down, contamination from bottom echoes usually biases velocity data toward zero. In a moving vessel, contamination from bottom echoes is less predictable. When looking up, contamination from surface echoes is unpredictable as a result of surface waves and winds, but a bias toward

zero is common. The velocity of the surface or the bottom is zero on average; it is this zero velocity that biases the measured velocity toward zero.

Ringing

Ringing is an effect in which energy from the transmit pulse lingers after the transmit pulse is finished. If there were no ringing, the transducer could receive echoes immediately after transmitting. However, echo signals are weak and it does not take much ringing to contaminate the echoes. Thus, the ADCP must wait for the ringing to die away before it can listen to and process the echoes. This waiting time is called the blanking period. Table 3 shows typical ringing times. These ringing times are approximately equal to the default blanking period.

Table 3. Typical ringing times, expressed as distances in front of the transducer.

Frequency	Ringing distance
75 kHz	6 m
150 kHz	4 m
300 kHz	2 m
600 kHz	1 m
1200 kHz	0.5 m

Ringing biases velocity data toward zero velocity because the ringing signal is not Doppler-shifted. Sources of ringing include:

- Receiver electronics
- Transducer and/or electronics housing
- Sea chest in a ship
- Ship's hull

In general, plastic housings ring less than metal housings. Sea chests covered with acoustic windows reflect sound around inside and thus cause greater ringing. Ringing is a problem in low backscatter because the ringing energy stays above the weak echo signals longer.

Ringing tends to be a more serious problem on ships than in other applications. You can minimize ringing in ships by taking the following steps:

- Mount the transducer on a material with a large acoustic impedance mismatch between the metal transducer and the metal hull. This reduces the sound energy that gets into the hull. (Note: be careful when choosing material for acoustic impedance. Some common materials, such as syntactic foam, that would appear to mismatch water's acoustic impedance are, in fact, surprisingly close!).
- Line sea chests with acoustically-absorbent material to attenuate sound bouncing around inside the sea chest.
- When acoustic windows are used, choose window materials that match the water's acoustic impedance to help minimize reflections within the sea chest.

TRDI provides a test program to measure ringing in vessel-mounted ADCPs.

Pressure

TRDI direct-reading and self-contained transducers are designed to withstand full-ocean-depth pressures. Our limited experience at depths greater than 2000 meters suggests that the transducer's performance is relatively unaffected, but that low backscatter tends to reduce range.

Concave vs. Convex

Self-Contained and Direct-Reading ADCPs use convex transducers (Figure 26) to allow the ADCP to be mounted in an in-line mooring cage. Vessel-Mounted ADCP transducers are concave to allow them to be mounted inside the smallest possible sea chest in the ship's hull.

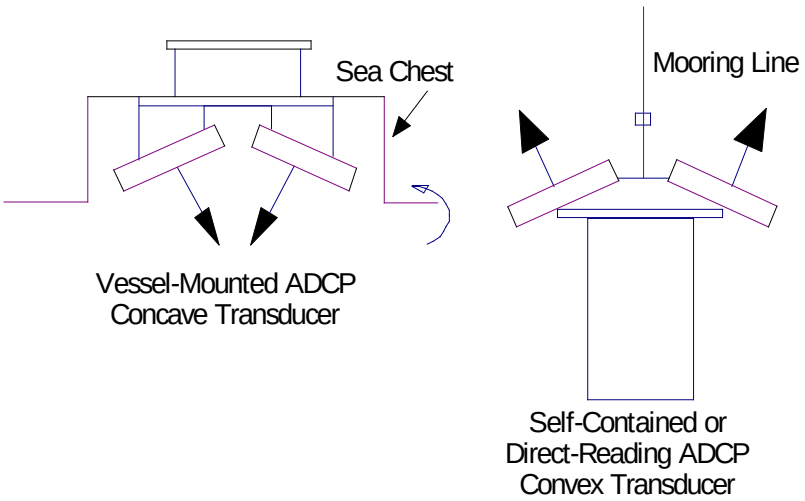

Figure 26. Concave and convex transducers.

12. Sound Speed and Thermoclines

This section addresses the effects of depth variations in sound speed and of thermoclines on data quality. Neither significantly impair data quality.

Sound Speed Variation with Depth

Variation of sound speed with depth does not affect measurement of *horizontal* currents. In simple terms, sound speed variation has two effects that exactly counteract one another. The effect of changing sound speed is to refract or bend the sound beams, but the bend is exactly the right amount to preserve the accuracy of the horizontal current (Figure 27).

The theoretical basis for this result is Snell's law, which says that horizontal wavenumber is conserved when sound passes through horizontal interfaces. Figure 27 shows that sound waves are continuous across the horizontal interface. Because the frequency remains constant, sound speed variation does not affect the horizontal component of sound velocity. And because measurement of the horizontal current depends directly on the horizontal sound speed, the horizontal current measurement is unaffected.

In contrast, variations in the *vertical* velocity component *are* proportional to variations in sound speed.

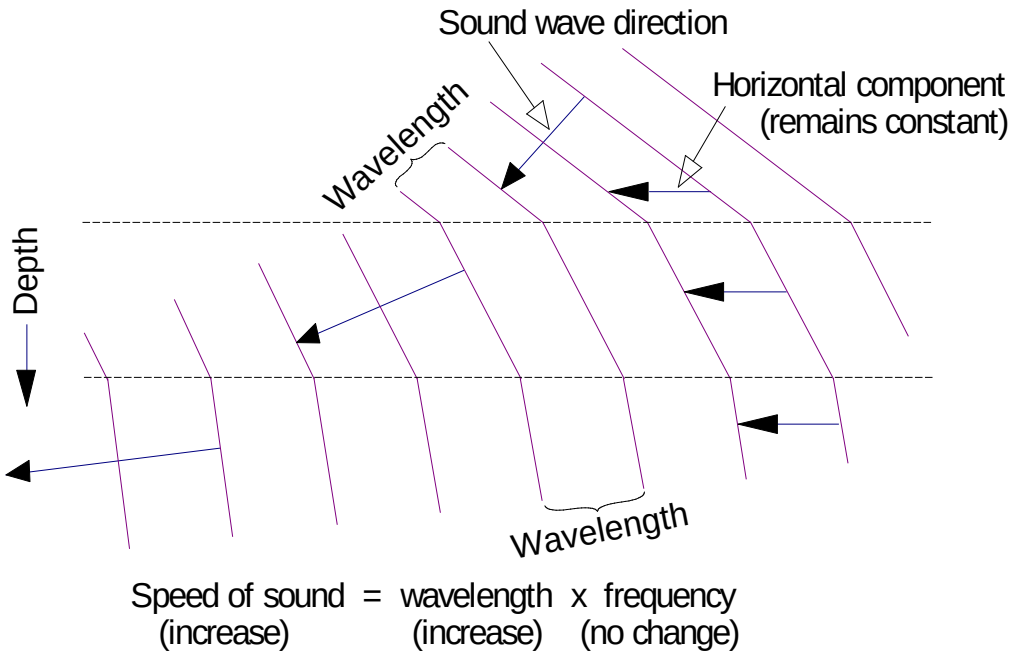

Figure 27. How sound speed variations with depth affects sound propagation. Even though the sound wave direction changes with depth (via refraction), the horizontal sound velocity remains constant.

Thermoclines

While strong thermoclines sometimes block sonar penetration, ADCPs can always penetrate the thermocline. The reason ADCPs can always penetrate the thermocline is that their beams are relatively steep, pointing more vertical than horizontal. Sonars that have trouble penetrating the thermocline have beams that are closer to horizontal. Such difficulties arise, for example, when a ship is trying to find a submarine near the thermocline (Figure 28).

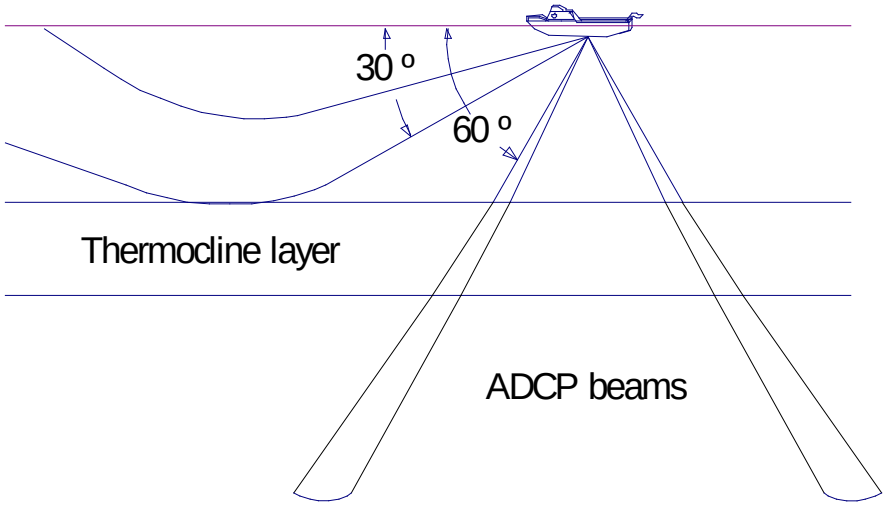

Figure 28. The effect of strong thermoclines on sound propagation.

13. Bottom Tracking

Most of this primer addresses water velocity profiling. This section describes how bottom-tracking compares to velocity profile measurements and how bottom-tracking is implemented.

Difference Between Bottom-Tracking and Water-Profiling

While water-profiling uses short transmit pulses to obtain vertical resolution, bottom-tracking requires long pulses. Long pulses are used to allow the sound beam to ensonify the bottom over the entire beam all at once (Figure 29). If the pulse is too short, the echo returns first from the leading edge of the beam, followed later by the trailing edge. Because the beam has a finite beamwidth, the angle of the beam relative to horizontal is different on these two edges. This means that the Doppler shift is different from one side of the beam to the other. By illuminating the bottom across the beam all at once, a long pulse produces an accurate and stable estimate of velocity, more accurate than is typically obtained from water profiles.

The downside of long transmit pulses is that a considerable part of the echo can come from water-mass echoes. Where water-mass echoes are weak relative to the bottom echo, this causes no problem, but in places with high concentrations of suspended sediment (i.e. in some rivers) the water-mass echoes can introduce significant *water bias* — this biases the bottom-track velocity toward the water velocity.

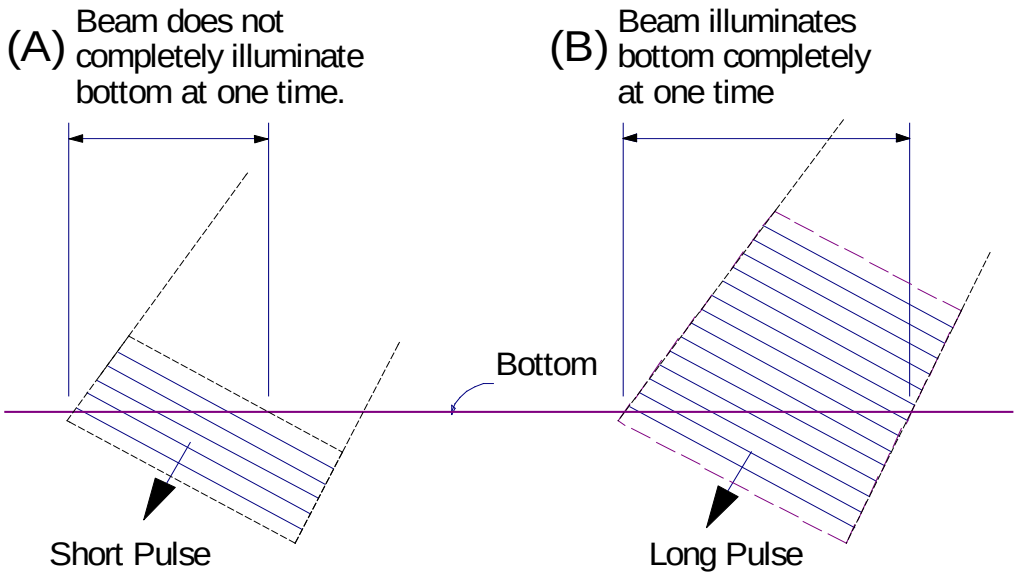

Figure 29. A long pulse is needed for the beams to ensonify (illuminate) the entire bottom all at once.

Implementation

Bottom tracking is implemented using separate pings from water profiling. The transmit pulse is longer, and the echo is processed in a different way. The bottom-track profile is divided into as many as 128 depth cells, each shorter than the transmit pulse (in contrast to water profiling). The ADCP searches through these depth cells to find the center of the echo and uses the center part to compute the Doppler shift. The ADCP also searches backward from beyond the bottom echo to find the echo's trailing edge. Because of the ADCP's slanting beams, this trailing edge provides a sharper and more accurate estimate of the bottom depth than the leading edge of the echo.

Accuracy and Capability

Bottom tracking has a typical single-ping accuracy of a few mm/s. The depth resolution is approximately 0.1 meter. The range capability is generally 50% greater than the water-profiling range.

Ice Tracking

An ADCP mounted on the seabottom can look up to track ice motion using its bottom-tracking capability (Belliveau, et al., 1989). Ice tracking requires that the ice be an unbroken sheet.

14. Phased Array Transducer

ADCP transducers are designed and manufactured so that the beams are transmitted at the proper angle. This is necessary to be able to calculate the true horizontal and vertical velocity components properly. TRDI manufactures two types of transducer assemblies for ADCPs: a piston transducer with 4 individual ceramic assemblies oriented at specific, fixed angles, and a phased-array transducer with single ceramic assembly. Both transducer designs simultaneously produce 4 acoustic beams at specific, fixed angles, but the phased-array creates all of the beams electronically from a single aperture, instead of from 4 separate apertures. One significant advantage is the greatly reduced overall size of the transducer at some particular frequency, employing the single-aperture phased array as compared to four independent piston transducers. This size comparison is demonstrated in Figures 1 and 2.

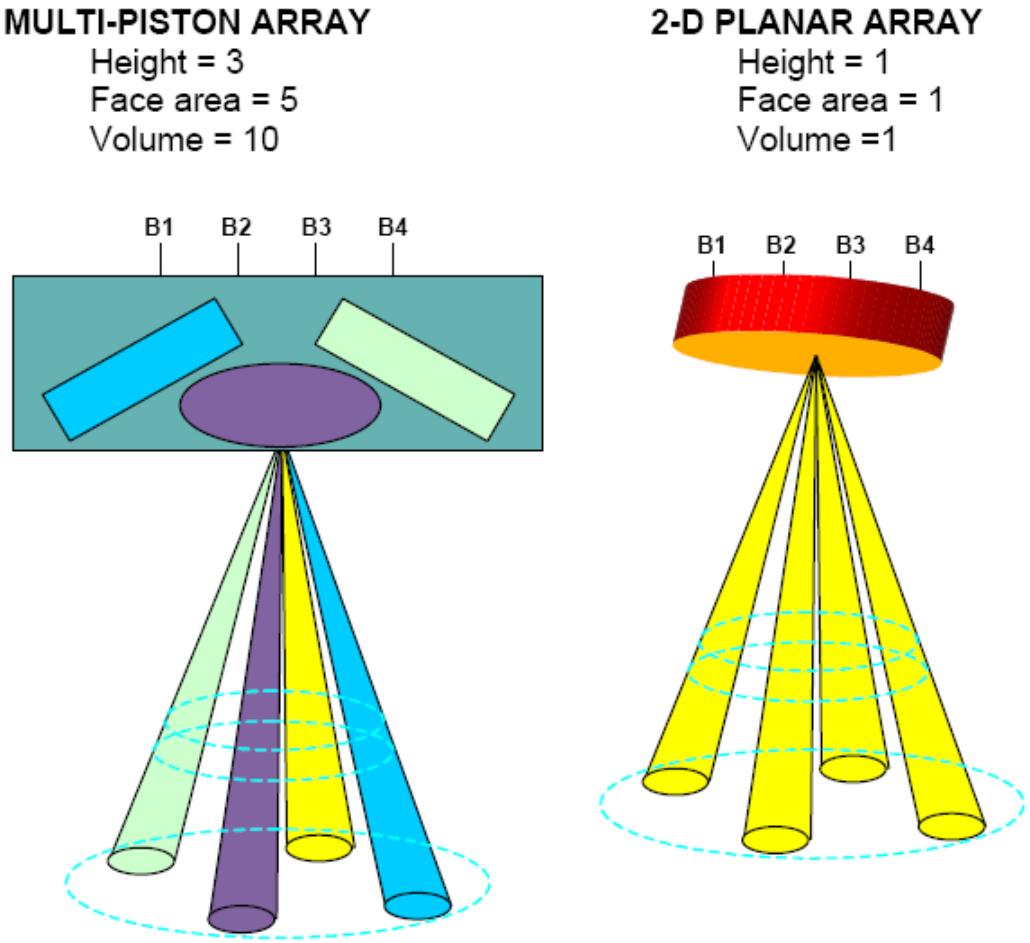

Figure 30. Comparison of a multi-piston and a 2-dimensional phased array transducer.

Figure 31. Comparison of a 600kHz developmental phased array transducer with a standard four piston 600kHz WorkHorse transducer.

Speed of sound considerations

Another advantage of the phased-array is that its measurement of horizontal (*x* and *y*) velocity components is independent of the speed of sound in the water. This is a fortunate consequence of the way the beams are formed. Phased-arrays use an electronic beamformer to introduce a time delay between successive elements in the array, producing a complex wave pattern that results in creating four separate beams similar in shape and orientation to those formed by four separate transducers.

Each element in the array is driven with the same signal except for a phase shift. The phase shift between elements is constant for a given frequency and element spacing. Therefore, if the speed of sound changes the beam angle will change. It can be shown (see the Phased-array Application Note) that for a Doppler measurement system, this turns out to be an advantage because the same ratio of change occurs in the Doppler shift equation. That is, the change in the Doppler frequency shift of the echo from a particle moving parallel to the face of the transducer array is compensated by a corresponding beam angle shift, rendering the horizontal velocity component independent of the speed of sound, thus requiring no correction. The vertical (*z*) velocity scale factor for the phased array, on the other hand, is somewhat *more* sensitive to sound speed changes than for the ordinary transducer. Therefore, a scale factor for the vertical velocity profile is recorded in the ADCP leader data, calculated based on the temperature sensor in the ADCP.

Summary

There are two principal advantages of a phased-array transducer over a conventional four piston transducer for an ADCP; greatly reduced size and weight, and horizontal velocity measurement independence of changes in the speed of sound.

15. Conclusion

We hope the information presented here will help you use ADCPs more effectively. If you have further questions about ADCP operation and design, contact Teledyne RD Instruments.

16. Useful References

Adler, M. (1993) Messungen von durchflüssen und strömungsprofilen mit einem ultraschall-Doppler gerät (ADCP), **Wasserwirtschaft, 83**, 192-196.

Appell, G. and P. Bass (1990) Near-surface measurements with a Doppler current profiler, **Proceedings of the IEEE Fourth Working Conference on Current Measurement,** April 3-5, 1990, Clinton, Maryland, 226-230.

Appell, G. F., J. Gast, R. G. Williams and P. D. Bass (1988) Calibration Of Acoustic Doppler Current Profilers, **Oceans '88 Proceedings**, IEEE Washington, DC, IEEE Catalogue number 88-CM2585-8, 346-352.

Appell, G. F., P. D. Bass and M. A. Metcalf (1991) Acoustic Doppler Current Profiler performance in near surface and bottom boundaries, **J**. **Oceanic Eng., OE-16**, 390-396.

Belliveau, D.J., G.L. Bugden, and S.G.K. Melrose (1989), Measurement of sea ice motion using bottom mounted Acoustic Doppler Current Profilers, **Sea Technology, 30**, February, 1989, 10-12.

Berezutskii A. V., S. E. Maximov, V. E. Sklyarov and R. L. Gordon (1991) Deep ADCP velocity measurements in the Gulf Stream, **J. Atmos**. **Oceanic Technol., 8**, 884-887.

Brumley, B. H., R. G. Cabrera, K. L. Deines and E. Terray (1991) Performance of a BroadBand Acoustic Doppler Current Profiler, **J. Oceanic Eng., OE-16**, 402-407.

Candela, J., R. C. Beardsley and R. Limeburner (1992) Separation of tidal and subtidal currents in ship-mounted Acoustic Doppler Current Profiler observations, **J. Geophys. Res., 97**, 767-788.

Clay, P., S. Kery, C. H. Robinson and J. Romeo (1990) Trawl-resistant, bottom-mounted, gimbaled 75-kHz Acoustic Doppler Current Profiler, **MTS '90 Proceedings**, Washington, DC, **2**, 348-352.

Firing, E. and R. L. Gordon (1990) Deep ocean Acoustic Doppler Current Profiling, **Proceedings of the IEEE Fourth Working Conference on Current Measurement**, April 3-5, 1990, Clinton, Maryland, 192-201.

Fischer, J. and M. Visbeck (1993) Deep velocity profiling with self-contained ADCPs, **J. Atmos**. **Oceanic Technol., 10**, 764-773.

Flagg, C. N. and S. L. Smith (1988) Use of the Acoustic Doppler Current Profiler to measure zooplankton abundance, **Deep-Sea Res., 36**, 455-474.

Flagg, C. N. and S. L. Smith (1989) Zooplankton abundance measurements from Acoustic Doppler Current Profilers, **Oceans '89 Proceedings**, IEEE Seattle, WA, IEEE Catalogue number 89-CH2780-5, 1318-1328.

Foreman, M. G. G. and H. J. Freeland (1991) A comparison of techniques for tide removal from ship-mounted Acoustic Doppler measurements along the southwest coast of Vancouver Island, **J. Geophys. Res., 96**, 17007-17021.

Gargett, A. E. (1994) Observing turbulence with a modified Acoustic Doppler Current Profiler, **J. Atmos**. **Oceanic. Technol., 11**, 1592-1610.

Geyer, R. W. (1993) Three-dimensional tidal flow around headlands, **J. Geophys. Res., 98**, 955-966.

Geyer, R. W., R. C. Beardsley, J. Candela, B. M. Castro, R. V. Legeckis, S. J. Lentz, R. Limeburner, L. B. Miranda and J. H. Trowbridge (1991) The physical oceanography of the Amazon outflow, **Oceanography, 4**, 8-14.

Gordon, R. L. (1989) Acoustic measurement of river discharge, **J. Hydraulic Eng., 115**, 925-936.

Gordon, R. L., A. V. Berezutskii, A. Kaneko, C. Stocchino and R. H. Weisberg (1990) A review of interesting results obtained with Acoustic Doppler Current Profilers, **Proceedings of the IEEE Fourth Working Conference on Current Measurement**, April 3-5, 1990, Clinton, Maryland, 180-191.

Griffiths, G. (1993) Improved underway ADCP data quality through precise heading measurement, **UK WOCE Newsletter, 11**, November 1993.

Joyce, T. M. (1989) On in-situ 'calibration' of shipboard ADCPs, **J. Atmos**. **Oceanic Technol., 6**, 164-172.

Kaneko, A., W. Koterayama, H. Honji, S. Mizuno, K. Kawatate and R. L. Gordon (1990) Cross-stream survey of the upper 400-m of the Kuroshio by an ADCP on a towed fish, **Deep-Sea Res., 37**, 875-889.

King, B. A. and E. B. Cooper (1994) GPS & DGPS: Navigation tools for shipboard ADCPs, **Sea Technology, 35,** March 1994.

Kinsler, L. E., A. R. Frey, A. B. Coppins and J. V. Sanders (1980) **Fundamentals of Acoustics, Third Edition**, John Wiley and Sons, New York.

Klein, H. and E. Mittelstaedt (1993) Local currents at a shoreface-connected ridge in the German bight, **Dt. Hydrogr. Z., 44**, 133-142.

Krogstad, H. E., R. L. Gordon and M. C. Miller (1988) High resolution directional wave spectra from horizontally mounted Acoustic Doppler Current Meters, **J. Atmos**. **Oceanic Technol., 5**, 340-352.

Leaman K. D., R. J. Findley and R. L. Hutchinson (1989) ADCP hull-mount comparisons alleviate acoustic problems, **Sea Technology, 30**, September 1989.

Magnell, B. (1990) Superduck: Performance of an Acoustic Doppler Current Profiler in a shallow-water wave environment, **Proceedings of the IEEE Fourth Working Conference on Current Measurement**, April 3-5, 1990, Clinton, Maryland, 225.

McPhaden, M. J., H. B. Milburn, A. I. Nakamura and A. J. Shepherd (1990) Proteus - Profile telemetry of upper ocean currents, **MTS '90 Proceedings**, Washington, DC, **2**, 353-357.

Melrose S. K., B. Eid and S. Sinnis (1989) Verification of sea-ice velocity measurements obtained from an Acoustic Doppler Current Profiler, **Oceans '89 Proceedings**, IEEE Seattle, WA, IEEE Catalogue number 89-CH2780-5, 1304-1307.

Muench, R. D., M. G. McPhee, C. A. Paulson and J. H. Morison (1992) winter oceanographic conditions in the Fram Strait-Yermak plateau region**, J. Geophys. Res., 97**, 3469-3483.

Muenchow, A., C. S. Coughran, M. C. Hendershott and C. Winant (1995) Performance and calibration of an Acoustic Doppler Current Profiler towed below the surface, **J. Atmos. Oceanic Technol., 12,** 435-444.

Murphy, D. J., D. C. Biggs and M. L. Cooke (1992) Mounting and calibrating an Acoustic Doppler Current Profiler, **MTS Journal, 26**, 34-38.

New, A. L. (1991) Factors affecting the quality of shipboard Acoustic Doppler Current Profiler data, **Deep-Sea Res., 39**, 1985-1996.

Oberg, K. A. and D. S. Mueller (1994) Recent applications of Acoustic Doppler Current Profilers, **Proceedings of the American Society of Civil Engineers Symposium, August 1-5, 1994, Buffalo, New York.**

Pettigrew, N. R., R. C. Beardsley and J. D. Irish (1986) Field evaluations of a bottom mounted Acoustic Doppler Profiler and conventional current meter moorings, **Proceedings of the IEEE Third Working Conference on Current Measurement**, January 22-24, 1986, Airlie, Virginia, 153-162.

Pollard R. and J. Read (1989) A method for calibrating shipmounted Acoustic Doppler Profilers and the limitations of gyro compasses, **J. Atmos**. **Oceanic Technol., 6**, 859-865.

Pulkkinen, K. (1993) Comparison of different bin-mapping methods for a bottom-mounted Acoustic Profiler, **J. Atmos**. **Oceanic Technol., 10**, 404-409**.**

Reichel G., H. P. Nachtnebel and P. Schreiner (1993) Zur Anwendung eines BB-ADCP in flachen Fliessgewaessern und Stauraeumen, Oesterreichische **Wasserwirtschaft, 45**, 25-35.

Robertson, K. G. and I. G. Chivers (1990) Acoustic Doppler Current Profiler installation and operation of a stemmed transducer system, **Proceedings of the IEEE Fourth Working Conference on Current Measurement**, April 3-5, 1990, Clinton, Maryland, 267-282.

Rowe, F. and J. Young (1979) An ocean current profiler using Doppler sonar, **Oceans '79 Proceedings.**

Rowe, F. D., K. L. Deines and R. L. Gordon (1986) High resolution current profiler, **Proceedings of the IEEE Third Working Conference on Current Measurement**, January 22-24, 1986, Airlie, Virginia, 184-189.

Schott, F. (1988) Effects of a thermistor string mounted between the acoustic beams of an Acoustic Doppler Current Profiler, **J. Atmos**. **Oceanic Technol., 5**, 154-159.

Schott, F. (1989) Measuring winds from underneath the ocean surface by upward looking Acoustic Doppler Current Profilers, **J. Geophys. Res., 94**, 8313-8321.

Schott, F. and K. D. Leaman (1991) Observations with moored Acoustic Doppler Current Profilers in the convection regime in the Gulfe du Lion, **J. Phys. Oceanogr., 21**, 558-57.

Schott, F. and W. Johns (1987) Half-year long measurement with a buoy-mounted Acoustic Doppler Current Profiler in the Somali Current, **J. Geophys. Res., 92**, 5169-5176.

Schott, F., K. D. Leaman and R. G. Zika (1988) Deep-mixing in the Gulf of Lions, **Geophys. Res. Letters, 15**, 800-803.

Schott, F., M. Visbeck and J. Fischer (1993) Observations of vertical currents and convection in the central Greenland Sea during the winter of 1988-1989, **J. Geophys. Res., 98**, 14401-14421..

Send, Uwe (1994) Accuracy of current profile measurement: effect of tropical and midlatitude internal waves, **J. Geophys. Res., 99**, 16229-16236.

Simpson, M. R. and R. N. Oltmann (1990) An acoustic Doppler discharge-measurement system, **Proceedings of the Hydraulic Engineering 1990 National Conference, 2**, 903-908.

Smith, J. (1993) Performance of a horizontally scanning Doppler sonar near shore, **J. Atmos**. **Oceanic Technol., 10**, 752-763.

Terray, E. A., H. E. Krogstad, R. Cabrera, R. L. Gordon and A. Lohrmann (1990) measuring wave direction using upward-looking Doppler sonar, **Proceedings of the IEEE Fourth Working Conference on Current Measurement**, April 3-5, 1990, Clinton, Maryland, 252-257.

Thomson, R. E., R. L. Gordon and A. G. Dolling (1991) An intense acoustic scattering layer at the top of a mid-ocean ridge hydrothermal plume, **J. Geophys. Res., 96**, 4839-4844.

Trump, C. L. (1989) Three practical hints on using vessel mounted ADCPs, **MTS Journal, 23**, 28-35.

Trump, C. L. (1991) Single ping ADCP data, **J. Oceanic Eng., OE-16**, 382-389.

Tubman, M.W. (1995) Plume Measurement System (PLUMES) Technical manual and data analysis procedures, Technical Report DRP-95-1, US Army Corps of Engineers, Vicksburg MS (Phone: 601-634-2355), 94 p.

Urick, R.J. (1983) **Principles of Underwater Sound, Third Edition**, McGraw-Hill, New York.

Visbeck, M. and J. Fischer (1995) Sea surface conditions remotely sensed by upward-looking ADCPs, **J. Atmos. And Oceanic Technol., 12**, 141-149.

Wilson, C. D. and E. Firing (1991) Sunrise swimmers bias acoustic Doppler, **Deep-Sea Res. , 39**, 885-892.

Winant, C., T. Mettlach and S. Larson (1994) Comparison of buoy-mounted 75-kHz Acoustic Doppler Current Profilers with vector measuring current meters, **American Meteorological Society, 11**, 1317-1333.

Yu, X. and L. Gordon (1995) 38 kHz BroadBand Phased Array Acoustic Doppler Current Profiler, **Proceedings of the IEEE Fifth Working Conference on Current Measurement**, February 7-9, 1995, St. Petersburg, Florida, 53-57.

Zedel, L. J. (1985) Evaluation of an Acoustic Doppler Profiler with application to stratified flow in a Fjord, M.S. Thesis, University of Victoria, Victoria, Canada.

Zedel, L. J. and J. A. Church (1987) Real-time screening techniques for Doppler current profiler data, **J. Atmos. and Oceanic Technol., 4**, 572-581.

Zedel, L. J., G. B. Crawford and R. L. Gordon (1996) On determination of wind direction using an upward looking ADCP, To appear in **J. Geophys. Res.**

Zhou, M., W. Nordhausen and M. Huntley (1994) ADCP measurements of the distribution and abundance of euphausiids near the Antarctic Peninsula in winter, **Deep-Sea Res., 41**, 1425-1445.

Index

A

acoustic windows, 39
ADCP coordinates, 18
ADCP data, 18
ADCP History, 1
ADCP tilt and depth cell mapping, 23
ambiguity, 11
Autocorrelation, 12
averaging over depth cells, 16
Averaging, ensemble, 20

B

backscatter coefficient, 29
backscattered sound, 6
  involves two Doppler shifts, 7
beam angle
  Depth cell mapping, 23
  Near-surface data, 38
beam coordinates, 23, 25
Beam coordinates, 18
beam pattern, 35
beam pattern, typical, 35
beam pointing errors, 25
Beam pointing errors, 21, 22
beam spreading, 29
Beam spreading, 31
Bias, 20, 21
bins. *See* depth cell
bottom echo, 38
bottom-track, 27, 28, 43, 44
Bottom-track, 27
Bottom-track data, 19
broadband ADCPs, 2
Broadband Doppler processing, 9
bubbles, 32

C

Cavitation, 32
cloud scatterers, 11
concave, 40
convex, 40
coordinate conversion matrix, 21
Correlation data, 19
current meter, 15
current profiles, 15
current, horizontal homogeneity, 13–14

D

data, 18
Data correction strategies, 24
data transmission time, 22
depth cell, 15, 16, 17, 21, 23, 24, 27, 29, 34, 44
  compared with conventional current meters, 15
Depth cell weight functions, 17
distribution of single-ping velocity data, 20
Doppler shift, 3, 5–11, 43–44

E

earth coordinates, 24
Earth coordinates, 18
echo intensity, 29
Echo intensity, 29
  data, 19
ensemble average, 20–22
error velocity, 14
Error velocity, 14
errors, 20–21

F

flux-gate compass, 24

G

Gyro errors and instability, 28

H

horizontal acceleration and tilt, 24–25
horizontal homogeneity, 13–14, 14

I

Ice tracking, 44
inclinometers, 24
Inclinometers, 24

J

Janus configuration, 14

L

layer of no motion, 27
Long-term uncertainty, 21

M

modes, 12
multiple beams, 13
multiple-turn synchros, 26

N

navigation, 27–28
Non-homogeneous flow leads to large error velocity, 14

O

obstructions in front of the transducer, 37

Obstructions, transducer clearance, 37

P

Parallel Velocity, 8
Percent-good data, 19
phase, 9–11
phased-array, 45
pitch and roll correction, 27
power, 31
pressure, 40
processing time, 22
propagation delay, 9–10, 12

R

radial motion, 8
random error, 20–21
Range gating, 16
range-dependent signal attenuation, 31
range-time plot, 16
redundancy, 14
reference layer, 27
Regular spacing, 15
relative motion, 8
Ringing, 39

S

scatterers, 6, 32
sea surface, echo, 38
Ship coordinates, 18
ship velocity, 27
ship's attitude data, 25
Shock, 32
short-term error, 21
Side lobes, 35
Snell's law, 41
Sound, 4
Sound absorption, 29–30
sound scatterers, 6, 32
sound speed, 33–34, 41
standard deviation, 20–21
synchro interface, 26

T

thermoclines, 42
tilt and depth cell mapping, 23
time dilation, 9–10
time lag, 10–12
transducer beam angle and the surface, 38
Transducer efficiency, 31
Transducer misalignment, 28
transducers, 35–40
  face view, 18
Transmit pulse, 32

V

Vector averaging, 22
Velocity data, 18

W

water bias, 43
weight function, 17

Notes

Notes